

DOE/AL/21557--T13

DE89 015784

CALCULATION OF THE OPTICAL POWER PROFILE FOR A SOLAR BOWL WITH AN IRIS ¹

Ronald M. Anderson Mandri Obeyesekere
Department of Mathematics Texas Tech University
Lubbock, Texas

May 15, 1987

¹DOE Contract No. DE-AC04-83AL21557

DISCLAIMER

This report was prepared as an account of work sponsored by an agency of the United States Government. Neither the United States Government nor any agency thereof, nor any of their employees, makes any warranty, express or implied, or assumes any legal liability or responsibility for the accuracy, completeness, or usefulness of any information, apparatus, product, or process disclosed, or represents that its use would not infringe privately owned rights. Reference herein to any specific commercial product, process, or service by trade name, trademark, manufacturer, or otherwise does not necessarily constitute or imply its endorsement, recommendation, or favoring by the United States Government or any agency thereof. The views and opinions of authors expressed herein do not necessarily state or reflect those of the United States Government or any agency thereof.

DISCLAIMER

Portions of this document may be illegible in electronic image products. Images are produced from the best available original document.

Contents

1	Introduction	1
2	Effective Aperture Calculations	3
2.1	Introduction	3
2.2	Spherical Segment Bowl	3
2.3	Spherical Segment Bowl with Iris	5
3	Spillage Calculations for Shallow Bowls	12
3.1	Introduction	12
3.2	Ray Tracing Geometry	13
3.3	Spillage Geometry	17
4	Finite Sun Concentration for a Spherical Mirror	27
4.1	Introduction	27
4.2	Geometrical Considerations	29
4.3	Shading and Rim Cutoff Effects	34
5	Solar Bowls with an Iris	36
5.1	Introduction	36
5.2	Determination of Rim-cutoff Angles for a Spherical Segment Bowl	38
5.3	Extension to Bowl with Iris	39
5.4	An Example	43
6	Optical Concentration Results	46
A	ROSAIRIS Program Listing	59

Abstract

This report develops analytical techniques for studying shallow spherical segment bowls that have an attached tracking iris. The report extends previous analytical models that were developed as part of the Crosbyton Solar Power Project for the case of spherical segment bowls.

Three types of calculations are considered. First, effective aperture formulas are derived for a spherical segment bowl with an iris, and results are compared with the bowl without an iris. Secondly, analytical formulas are derived to determine spillage losses for shallow bowls. Finally, the powerful **Ratio of Solid Angles (ROSA)** computer code is extended to include solar profiles for a spherical segment bowl with iris.

The report includes several plots comparing optical power concentration ratios for solar bowls with and without an iris. A complete listing of the extended code, **ROSAIRIS**, is given in the appendix.

List of Figures

2.1	Solar Bowl Geometry	4
2.2	Orthogonal Projection of Rim onto Reference Plane	6
2.3	Geometrical Parameters for a Solar Bowl with Iris.	7
2.4	Comparison of Spherical Segment Bowls and a 30° Bowl with an Iris.	11
3.1	Geometry for Single Bounce Rays	14
3.2	Multiple Bounce Geometry ($n = 3$)	16
3.3	Receiver Reception Point vs Impact Angle	18
3.4	Side View of Spillage Geometry	20
3.5	Overhead View of Spillage Geometry	21
3.6	Spillage vs Inclination Angle (30° bowl and unit solar insolation).	24
4.1	Geometry for Integration	30
4.2	Solid Angle Geometry for a Finite Solar Disk	31
4.3	The Intersection of a Constant ω -plane with the Sun Cone.	33
4.4	Rim Cutoff Effects	35
5.1	Angles Used in Rim-cutoff Calculations	37
5.2	Location of the Sun in the <i>SEV</i> -system	40
5.3	The <i>SEV</i> and <i>DMA</i> Coordinate Systems	41
5.4	Location of the <i>D'M'A</i> Coordinate System	42
5.5	Intersection of the ω -plane with the Rim	45
6.1	Comparison of Input Energy and Captured Energy	47
6.2	Optical Power Concentration for $I = 00^\circ$ and $\theta_R = 30^\circ$, $\theta_I = 45^\circ$, $\phi_0 = 45^\circ$	48

6.3	Optical Power Concentration for $I = 10^\circ$ and $\theta_R = 30^\circ$, $\theta_I = 45^\circ$, $\phi_0 = 45^\circ$	49
6.4	Optical Power Concentration for $I = 20^\circ$ and $\theta_R = 30^\circ$, $\theta_I = 45^\circ$, $\phi_0 = 45^\circ$	50
6.5	Optical Power Concentration for $I = 30^\circ$ and $\theta_R = 30^\circ$, $\theta_I = 45^\circ$, $\phi_0 = 45^\circ$	51
6.6	Optical Power Concentration for $I = 40^\circ$ and $\theta_R = 30^\circ$, $\theta_I = 45^\circ$, $\phi_0 = 45^\circ$	52
6.7	Optical Power Concentration for $I = 50^\circ$ and $\theta_R = 30^\circ$, $\theta_I = 45^\circ$, $\phi_0 = 45^\circ$	53
6.8	Optical Power Concentration for $I = 60^\circ$ and $\theta_R = 30^\circ$, $\theta_I = 45^\circ$, $\phi_0 = 45^\circ$	54
6.9	Optical Power Concentration for $I = 70^\circ$ and $\theta_R = 30^\circ$, $\theta_I = 45^\circ$, $\phi_0 = 45^\circ$	55
6.10	Optical Power Concentration for $I = 80^\circ$ and $\theta_R = 30^\circ$, $\theta_I = 45^\circ$, $\phi_0 = 45^\circ$	56

Chapter 1

Introduction

Previous analytical studies of solar profiles have concentrated on spherical segment bowls with a cylindrical or conical receiver. These studies use the **ROSA** (Ratio of Solid Angles) method of Reichert and Brock [1,2,3]. The method was first applied to the case of an aligned, conical receiver and a spherical segment mirror [1]. The results were then extended to account for misalignment of the receiver in [4,5] and to other shaped receivers in [6,7].

In this report, we extend the previous results to include solar profiles for a spherical segment bowl with a tracking reflector mounted on its rim. This concept was introduced by the French [8] for a 60° bowl and was called a 'visor'. The term 'iris' is used in the Crosbyton Solar Power Project for such a mounted, tracking reflector.

In the solar bowl concept, the reflecting surface is fixed and the receiver tracks the sun. Because the aperture plane of the bowl is fixed, the total power captured by the bowl falls off as $\cos I$, where I is the inclination angle of the sun relative to the axis of symmetry of the bowl. The addition of the tracking iris modifies this cosine loss and thereby increases the total annual power captured by the solar bowl. A complete study of the economics of adding an iris to a solar bowl requires that the increased annual power output of the bowl be weighed against the increased construction and operational costs of the bowl with iris. This report will provide the mathematical background for such a study, but will not carry out the study.

The total solar energy entering a solar bowl with an iris can be calculated as a function of inclination angle, I , by considering the orthogonal

projection of the rim of the bowl onto an appropriate reference plane. These calculations are carried out in Section 2. In the case of shallow bowls, some of the energy entering the bowl cannot be captured by the receiver. This is because a portion of the multiple bounce rays may spill over the edge of bowl without striking the receiver. This loss of energy, called spillage, is discussed in Section 3.

The calculation of detailed point-by-point concentrations on the receiver is accomplished by application of the **ROSA** method. Section 4 gives a brief review of the application of the **ROSA** method for the case of a receiver in a spherical segment bowl. The method is extended to the case of an iris in Section 5. The modified program is named **ROSAIRIS**. A comparison of spherical segment bowl solar profiles and profiles for a spherical segment bowl with iris is presented in Section 6.

A detailed description of all coordinate systems used in the calculations, together with a derivation of all formulas, may be found in [[7]]. A listing of the **ROSAIRIS** computer code is included in Appendix A of this report.

Chapter 2

Effective Aperture Calculations

2.1 Introduction

This chapter presents results concerning the total energy entering a solar bowl as a function of the angle of inclination, I , of the sun relative to the axis of symmetry of the bowl. Results are presented for a spherical segment bowl and for a spherical segment bowl with an iris. The results are obtained by computing the orthogonal projection of the surface of the bowl unto a reference plane that is perpendicular to the direction of the sun.

2.2 Spherical Segment Bowl

The geometrical parameters for a spherical segment solar bowl are shown in Figure 2.1. The bowl has radius R and the angle θ_R is called the rim angle of the bowl. I denotes the inclination angle of the sun relative to the axis of symmetry of the bowl, i.e., I is the angle between the axis of symmetry of the bowl and the direction of the sun. We fix a reference plane above the bowl with normal direction pointing towards the sun. The perpendicular projection of the rim onto the reference plane forms an ellipse in the reference plane and all input power to the bowl passes through this ellipse. Thus, the total power entering the solar bowl is proportional to the

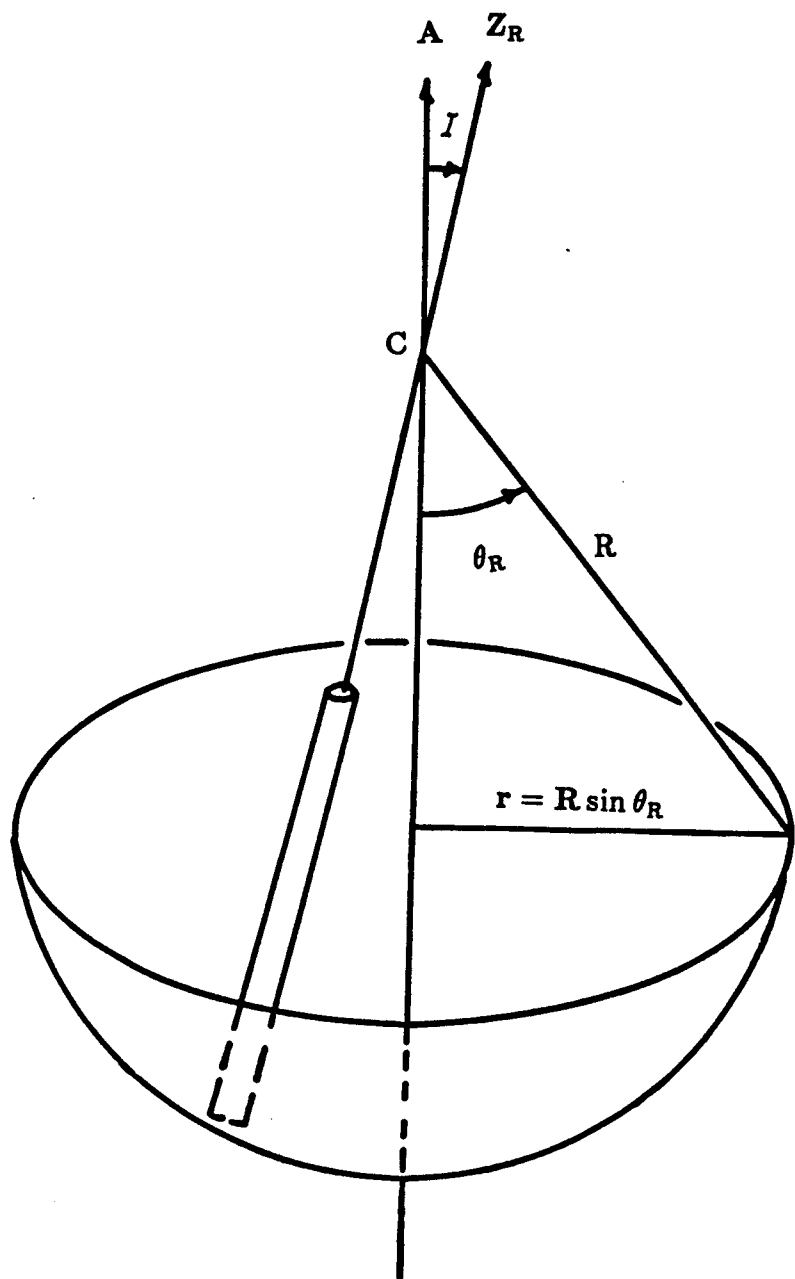


Figure 2.1: Solar Bowl Geometry

area of this ellipse. The projected area is given by

$$A_{\text{proj}} = \pi r^2 \cos I, \quad (2.1)$$

where $r = R \sin \theta_R$. This projected area gives the effective aperture of the bowl as a function of inclination angle I . This projection is illustrated in Figure 2.2.

Generally, the bowl is tilted to the south for locations in the northern hemisphere, and sun is located by an azimuth angle, \mathcal{A} and an elevation angle \mathcal{E} . \mathcal{A} is measured from the south axis and \mathcal{E} is measured from the horizontal plane. The angle between the vertical and the axis of symmetry is denoted by γ . In terms of these parameters, the inclination angle of the sun relative to the axis of symmetry of the bowl is given by

$$\cos I = \sin \gamma \cos \mathcal{E} \cos \mathcal{A} + \cos \gamma \sin \mathcal{E}. \quad (2.2)$$

2.3 Spherical Segment Bowl with Iris

For inclination angles of 90° or less, the effective aperture of a spherical segment bowl with an iris is simply the sum of the effective apertures of each part. In order to compute the effective aperture of the iris, we form the perpendicular projection of the iris onto the reference plane and calculate the projected area.

In order to carry out the calculations, we employ a collector fixed coordinate system (see Figure 2.3) with origin at the center of symmetry, C , of the bowl. The axes are called D , M , and A . The A axis is the symmetry axis of the spherical segment bowl, D is directed to the south and M to the east. Let e_s denote a unit vector pointing from C to the center of the sun, so that I is the angle between e_s and the A -axis. If $I \neq 0$ define a D' -axis by the projection of e_s onto the D - M coordinate plane, and define M' so that the D' - M' - A coordinate system forms a right hand system. If $I = 0$, we let D' -axis coincide with the D -axis. The surface of the iris can be expressed parametrically, using spherical coordinates, as

$$\begin{cases} D' &= R \cos \phi \sin \theta, \\ M' &= R \sin \phi \sin \theta, \\ A &= R \cos \theta, \end{cases} \quad (2.3)$$

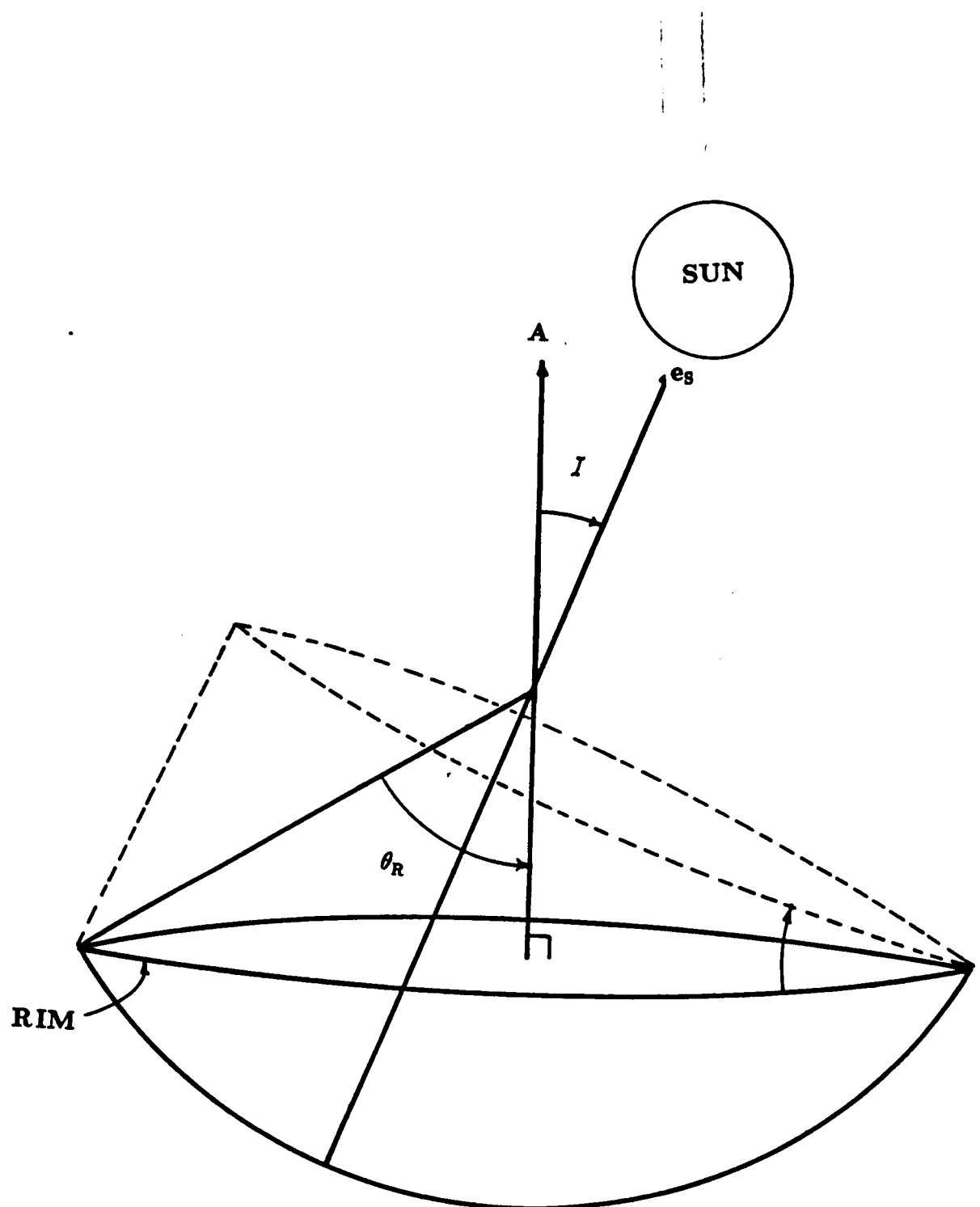


Figure 2.2: Orthogonal Projection of Rim onto Reference Plane

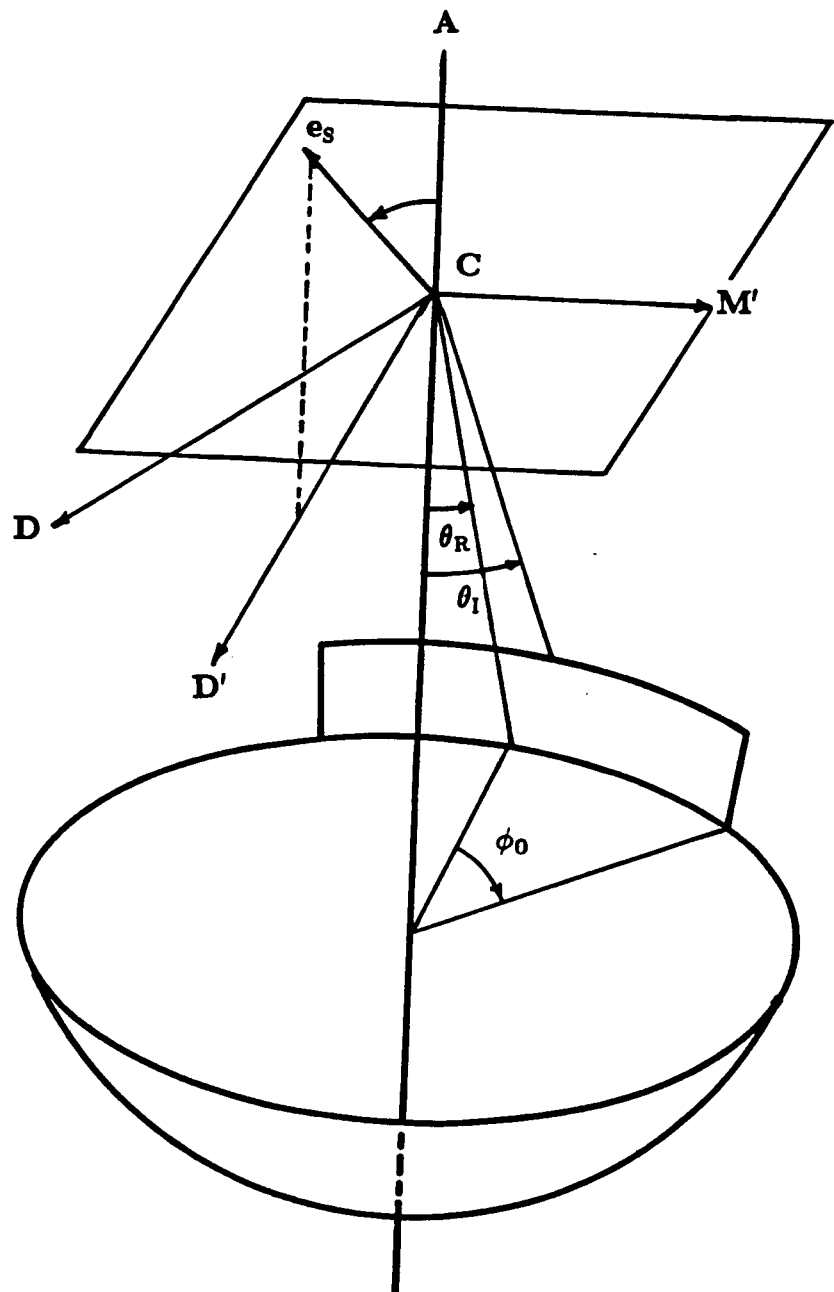


Figure 2.3: Geometrical Parameters for a Solar Bowl with Iris.

where θ is the zenith angle of a point on the iris, (measured from the A -axis), ϕ is an azimuthal angle measured from the D' -axis, and (ϕ, θ) lie in some set S in the ϕ - θ coordinate system. If the reference plane is horizontal, the iris projects onto the planar region with coordinates

$$\begin{cases} D' = R \cos \phi \sin \theta, \\ M' = R \sin \phi \sin \theta, \end{cases} \quad (2.4)$$

where $(\phi, \theta) \in S$.

In order to find the planar area for other orientations of the reference plane we rotate the reference plane through an angle I so that its normal has the direction of \mathbf{e}_s . We define a local x - y - z coordinate system with the x and y axes lying on the reference plane and the z axis having the direction of \mathbf{e}_s , i.e. pointing towards the sun. Because the iris tracks the sun, the projection of the iris will be symmetric relative to the x -axis in the reference plane. A point on the iris with coordinates (ϕ, θ) has rectangular coordinates (x, y, z) , with

$$\begin{pmatrix} x \\ y \\ z \end{pmatrix} = \begin{pmatrix} \cos I & 0 & -\sin I \\ 0 & 1 & 0 \\ \sin I & 0 & \cos I \end{pmatrix} \begin{pmatrix} R \cos \phi \sin \theta \\ R \sin \phi \sin \theta \\ R \cos \theta \end{pmatrix}.$$

The projection of this point onto the reference plane is given by

$$\begin{cases} x = R(\cos I \cos \phi \sin \theta - \sin I \cos \theta) \\ y = R \sin \phi \sin \theta. \end{cases} \quad (2.5)$$

The projected area is given by

$$A_{\text{proj}} = \iint_{\mathcal{R}} dx dy, \quad (2.6)$$

where \mathcal{R} is the region in the projected plane obtained from the orthogonal projection of the iris.

The above integral is evaluated by integration in the (ϕ, θ) variables. The mapping

$(\phi, \theta) \rightarrow (x, y)$ has Jacobian

$$J = R^2 \times \text{DET} \begin{pmatrix} -\cos I \sin \phi \sin \theta & \cos \phi \sin \theta \\ \cos I \cos \phi \cos \theta + \sin I \sin \phi & \sin \phi \cos \theta \end{pmatrix},$$

$$= -R^2(\cos I \sin \theta \cos \theta + \sin I \sin^2 \theta \cos \phi).$$

Thus,

$$\begin{aligned} A_{\text{proj}}(I) &= \iint_S |J| d\phi d\theta \\ &= R^2 \iint_S |\cos I \sin \phi \cos \phi + \sin I \sin^2 \theta \cos \phi| d\phi d\theta \quad (2.7) \end{aligned}$$

We illustrate these results for the case where the iris is defined by

$$\begin{cases} \pi - \phi_0 \leq \phi \leq \pi + \phi_0 \\ \pi - \theta_I \leq \theta \leq \pi - \theta_R. \end{cases} \quad (2.8)$$

The iris is illustrated on Figure 2.3. The projected area is given by

$$\begin{aligned} A_{\text{proj}}(I) &= 2R^2 \int_{\theta_R}^{\theta_I} \int_0^{\phi_0} [\cos I \sin \theta \cos \theta + \sin I \sin^2 \theta \cos \phi] d\phi d\theta \\ &= R^2 (\cos I [\sin^2 \theta_I - \sin^2 \theta_R] \phi_0 \\ &\quad + \sin I \sin \phi_0 [\theta_I - \theta_R - \frac{1}{2}(\sin 2\theta_I - \sin 2\theta_R)]) \quad (2.9) \end{aligned}$$

This area is added to the area given in Equation 2.1 to get the effective aperture of the bowl with iris. This gives

$$\begin{aligned} A_E &= R^2 (\cos I [\phi_0 \sin^2 \theta_I + (\pi - \phi_0) \sin^2 \theta_R] \\ &\quad + \sin I \sin \phi_0 [\theta_I - \theta_R - \frac{1}{2}(\sin 2\theta_I - \sin 2\theta_R)]) \quad (2.10) \end{aligned}$$

For comparison purposes, it is instructive to normalize the effective aperture of a bowl by dividing by its surface area. For a spherical segment bowl with rim angle θ_R , the surface area is given by

$$SA_{\text{bowl}} = 2\pi R^2 (1 - \cos \theta_R). \quad (2.11)$$

The surface area for the iris described in Eq. 2.8 is given by

$$SA_{\text{iris}} = 2R^2 [\pi - (\pi - \phi_0) \cos \theta_R - \phi_0 \cos \theta_I]. \quad (2.12)$$

Thus, the total surface area is given by

$$SA = R^2 [4\pi(1 - \cos \theta_R) + 2\phi_0(\cos \theta_R - \cos \theta_I)]. \quad (2.13)$$

The normalized effective aperture is then

$$NA_E = \frac{\cos I [\phi_0 \sin^2 \theta_I + (\pi - \phi_0) \sin^2 \theta_R] + \sin I \sin \phi_0 [\theta_I - \theta_R - (\sin 2\theta_I - \sin 2\theta_R)/2]}{4\pi(1 - \cos \theta_R) + 2\phi_0(\cos \theta_R - \cos \theta_I)}. \quad (2.14)$$

A plot of normalized effective aperture vs I is shown in Figure 2.4 for the case where $\theta_R = 30^\circ$, $\theta_I = 45^\circ$, and $\phi_0 = 45^\circ$. Curves are also shown for spherical segment bowls with $\theta_R = 30^\circ$ and $\theta_R = 60^\circ$. Note that the point where the effective aperture is maximum occurs at an inclination angle of near 10° as opposed to the 0° maximum for the cosine law curve for the spherical segment bowl.

The procedures discussed in the above example apply equally well to other iris shapes. In every case, the effective aperture of the iris is determined by evaluating the integral in Eq. 2.7. Only the description of the set S varies from case to case, and thus it is only necessary to determine the limits of integration in Eq. 2.7 and evaluate the resulting integral to treat a given iris shape.

The graphs shown in Figure 2.4 include values calculated by the ROSA computer code. The points marked by a "Δ" are computed values for the spherical segment bowl with an iris, and the points marked by "x" are values for a 30° bowl. The apparent discrepancies between theoretical and computed values arise for shallow bowls because of spillage losses for multiple bounce rays. These losses are discussed in the next chapter.

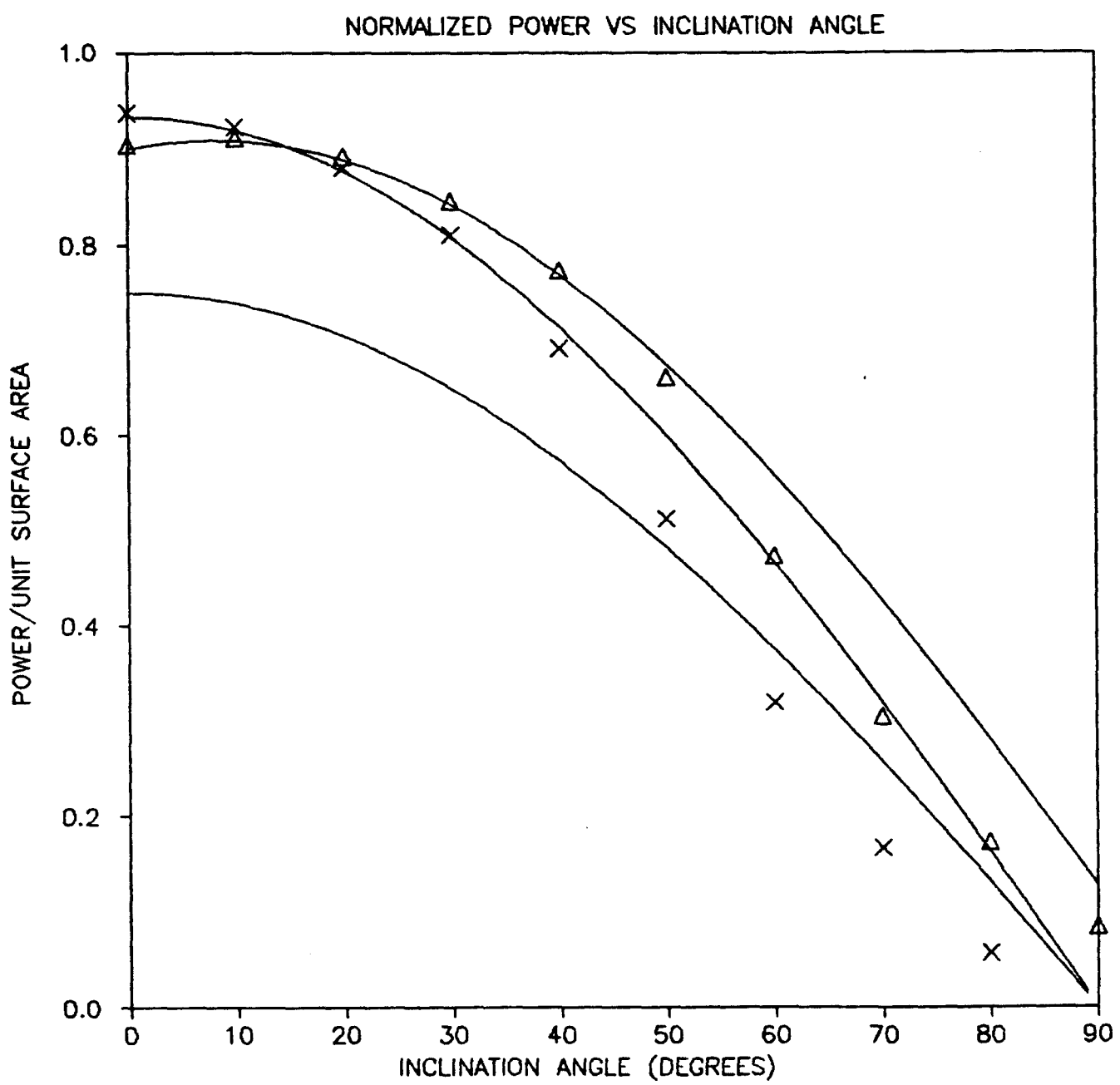


Figure 2.4: Comparison of Spherical Segment Bowls and a 30° Bowl with an Iris.

Chapter 3

Spillage Calculations for Shallow Bowls

3.1 Introduction

The previous chapter developed formulas for the amount of energy entering the bowl as a function of inclination angle of the sun. In the case of shallow bowls and large inclination angles, a part of this energy will not be captured by the receiver, even assuming a perfect mirror surface and a receiver that captures all energy striking it. This loss occurs at inclination angles where the lower end of the receiver is above the rim of the bowl. The last reflection of multiple bounce rays strikes the surface of the bowl near the foot of the receiver, and, when the foot of the receiver is above the rim of the bowl, the mirror support is missing. Thus, the receiver would have to be longer than the radius of the bowl in order to capture the ray. The loss of energy due to missing the multiple bounce rays is called *spillage*. It should be noted that this spillage does not occur for bowls such as the 60° bowl, because rim shadowing effects prevent these spillage losses at large inclination angles.

This chapter derives formulas for the loss of energy due to spillage of multiple bounce rays. The method treats the sun as a point sun at infinity and uses ray tracing to describe the path of a ray that is reflected from the spherical mirror surface prior to striking the receiver or spilling over the edge of the bowl. The ray tracing geometry is described in Section 3.2. Section 3.3 describes the method by which energy is lost in shallow bowls, and derives formulas for the loss of energy (again based on ray tracing).

Section 3.3 also gives a comparison of the results from ray tracing and the more exact results obtained from the ROSA computer code.

3.2 Ray Tracing Geometry

The general nature of the concentration profile due to reflection from a spherical segment mirror (bowl) can be deduced by considering a simple model based on a point sun at infinity. For this simplified situation, the sun's rays can be treated as parallel rays and the problem reduces to a two-dimensional geometry. The geometry is illustrated in Figure 3.1. In Figure 3.1, C denotes the center of a sphere of unit radius (all units are normalized). The receiver (boiler) is taken to be a right circular cylinder of radius a with axis along the z -axis and length 0.5. The z -axis is chosen to be parallel to the direction of rays from the sun, with origin at the center of the sphere. The positive direction of z is downward so that the receiver extends from $z = 0.5$ to $z = 1.0$. The location of a point Q on the receiver surface is specified by z and the zenith angle $\psi = \arctan a/z$.

To be received at Q, a ray from the sun must strike the mirror at a point P such that after reflection (n times) according to Snell's equal angle law, the ray path will pass through Q. The angle θ at which the ray strikes the mirror (the angle between the ray and PC) is called the *impact angle* of the ray, while the *reception angle*, β , is the angle of the incoming ray at Q as measured from the radius through CQ.

For a single bounce ray ($n = 1$), the law of sines, applied to the triangle CQP, gives:

$$\frac{(z/\cos\psi)}{\sin\theta} = \frac{1}{\sin\beta}, \quad (3.1)$$

where $\beta = 2\theta - \psi$ and $\tan\psi = a/z$. Elimination of β and ψ from Eq. 3.1 leads to the formula:

$$z = \frac{\sin\theta + a\cos(2\theta)}{\sin(2\theta)}. \quad (3.2)$$

The minimum value of z occurs when $\sin\theta = a^{1/3}$ and

$$z_{min} = \frac{1 + S(1 - 2S)}{2\sqrt{1 - S}}, \quad \text{where } S = a^{2/3}. \quad (3.3)$$

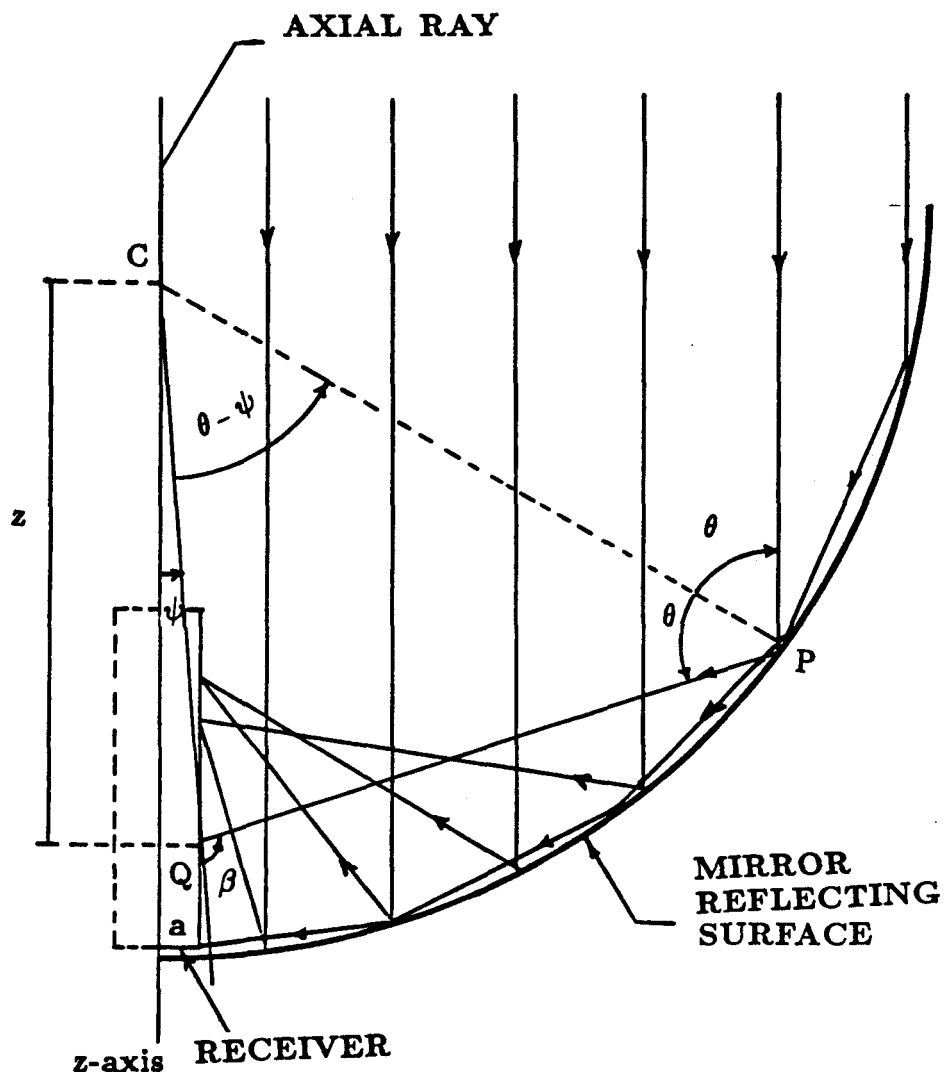


Figure 3.1: Geometry for Single Bounce Rays

In particular, for $a = 0$, $z_{min} = 0.5$. Thus the rays are focused on the receiver at locations in the range

$$z_{min} \leq z \leq \sqrt{1 - a^2}, \quad \text{with } z_{min} \geq 0.5. \quad (3.4)$$

An analysis of Eq. 3.2 also shows that z is an increasing function of θ for $\arcsin a \leq \theta \leq \arcsin a^{1/3}$ and increasing for $\arcsin a^{1/3} \leq \theta \leq \pi/3$. The value $\pi/3$ is obtained by considering the extreme case of $a = 0$ and $z = 1$. Thus, there exist exactly *two* impact angles which cause rays to strike the receiver at a given z coordinate on the cylinder.

Multiple reflections occur for impact angles greater than 60 degrees (i.e. greater than $\pi/3$ radians). The geometry for the case $n = 3$ is shown in Figure 3.2. A ray will be reflected n times before striking the receiver provided the impact angle θ satisfies

$$\frac{(n-1)\pi}{2n-1} + \frac{\psi}{2n-1} \leq \theta \leq \frac{n\pi}{2n+1} + \frac{\psi}{2n+1}. \quad (3.5)$$

Consideration of the triangle CPQ again yields Equation 3.2. The angle ψ can be eliminated and the resulting equation solved for z . The z -coordinate of the point where the ray strikes the receiver is given by

$$z = \frac{\sin \theta + a \cos \alpha_n}{\sin \alpha_n}, \quad (3.6)$$

where $\alpha_n = 2n\theta - (n-1)\pi$. A ray that is reflected n times strikes the receiver in the range

$$z_{min,n} \leq z \leq \sqrt{1 - a^2}. \quad (3.7)$$

The impact angle that yields $z_{min,n}$ is found from

$$(2n+1) \sin(2n-1)\theta - (2n-1) \sin(2n+1)\theta + 4na \cos n\pi = 0. \quad (3.8)$$

As n increases, $z_{min,n}$ approaches 1. Moreover, for each z in the focal region there exist exactly two impact angles which cause rays to strike the receiver at z . The two impact angles are the solutions, θ , to the transcendental equation

$$z \sin(2n\theta) + \cos(n\pi) \sin \theta = a \cos(2n\theta). \quad (3.9)$$

Figure 3.3 shows a plot of impact angle, θ , vs reception point, z . The bowl is taken to have a unit radius and a is normalized so that the ratio of

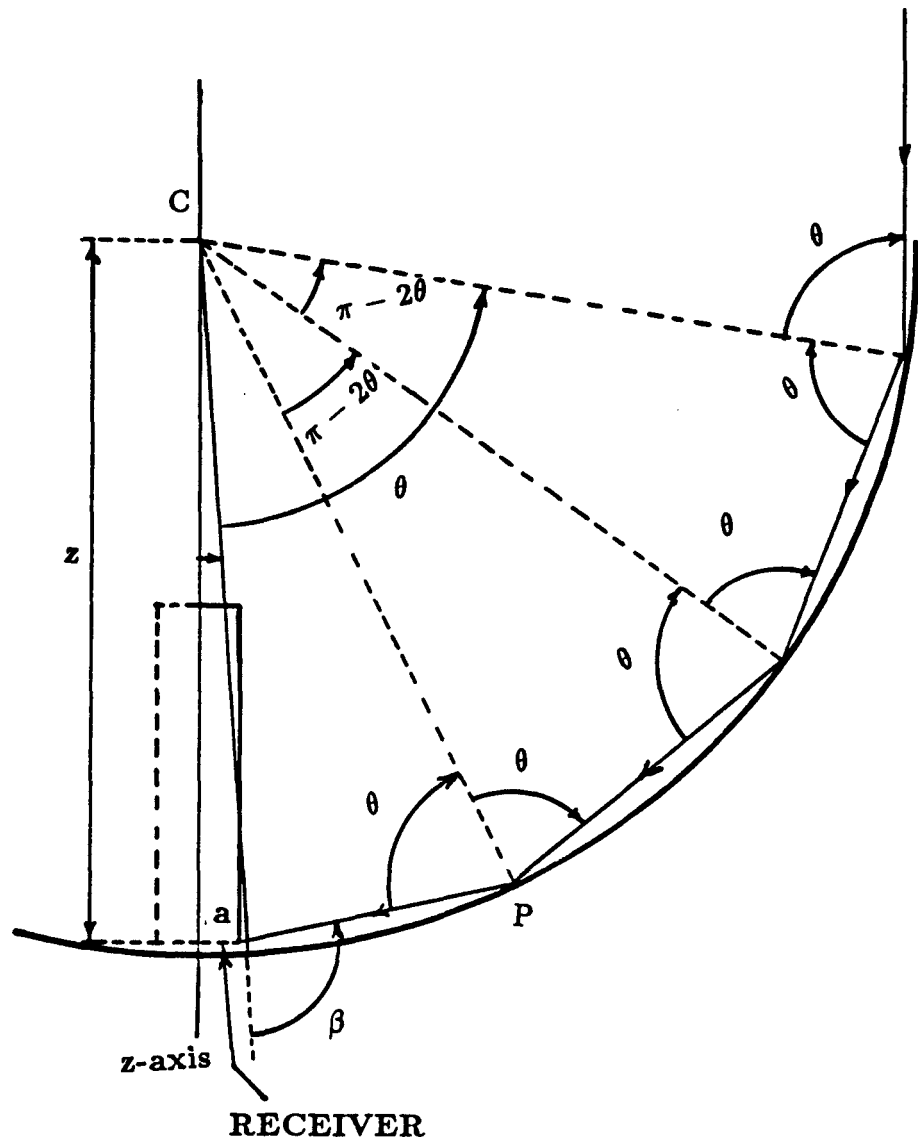


Figure 3.2: Multiple Bounce Geometry ($n = 3$)

the boiler radius to the bowl radius is the same as that at the Crosbyton Solar Power ADVS site. In the figure, the region from $\theta = 0^\circ$ to $\theta = 60^\circ$ is the region of single bounce rays, the region from $\theta = 60^\circ$ to $\theta = 72^\circ$ corresponds to two bounce rays, and so on.

3.3 Spillage Geometry

This section addresses the problem of spillage. We simplify the calculations by setting $a = 0$.

A ray that is reflected n times before striking the receiver is called a ray of order n . It follows from Equation 3.5 that a ray of order n has impact angle, θ , where

$$\frac{(n-1)\pi}{2n-1} < \theta \leq \frac{n\pi}{2n+1}. \quad (3.10)$$

A straightforward calculation also shows that the last reflection of a ray of order n occurs in the region

$$0 < \theta \leq \frac{\pi}{2n+1}. \quad (3.11)$$

The angle between the z -axis and the point where a ray of order n last strikes the bowl (the angle between the z -axis and the line CP in Figure 3.2) is given by

$$\theta_P = (n-1)\pi + (2n-1)\theta \quad (3.12)$$

We denote the upper and lower limits of the impact angles for rays of order n by the symbols θ_n^+ and θ_n^- , respectively, and the upper limit for the angle at which the last reflection occurs by θ_n^0 . Then, $\theta_n^+ = n\pi/(2n+1)$, $\theta_n^- = (n-1)\pi/(2n-1)$, and $\theta_n^0 = \pi/(2n+1)$.

Spillage occurs when the inclination angle of the sun relative to the axis of symmetry of the bowl is greater than the rim angle of the bowl, i.e, when $I > \theta_R$. A two dimensional view of spillage is illustrated in Figure 3.4. In this example, $I = 45^\circ$ and $\theta_R = 30^\circ$. Impact angles are measured relative to the z -axis (the receiver) and for this example we have $15^\circ \leq \theta \leq 75^\circ$. Thus, we have rays of order one, two, and three.

All rays of order one strike the receiver. Rays of order two have impact angles lying between $\pi/3$ and $2\pi/5$. They require mirror support in the region $0 < \theta_P < \pi/5$. However, no mirror support exists in the region $0 <$

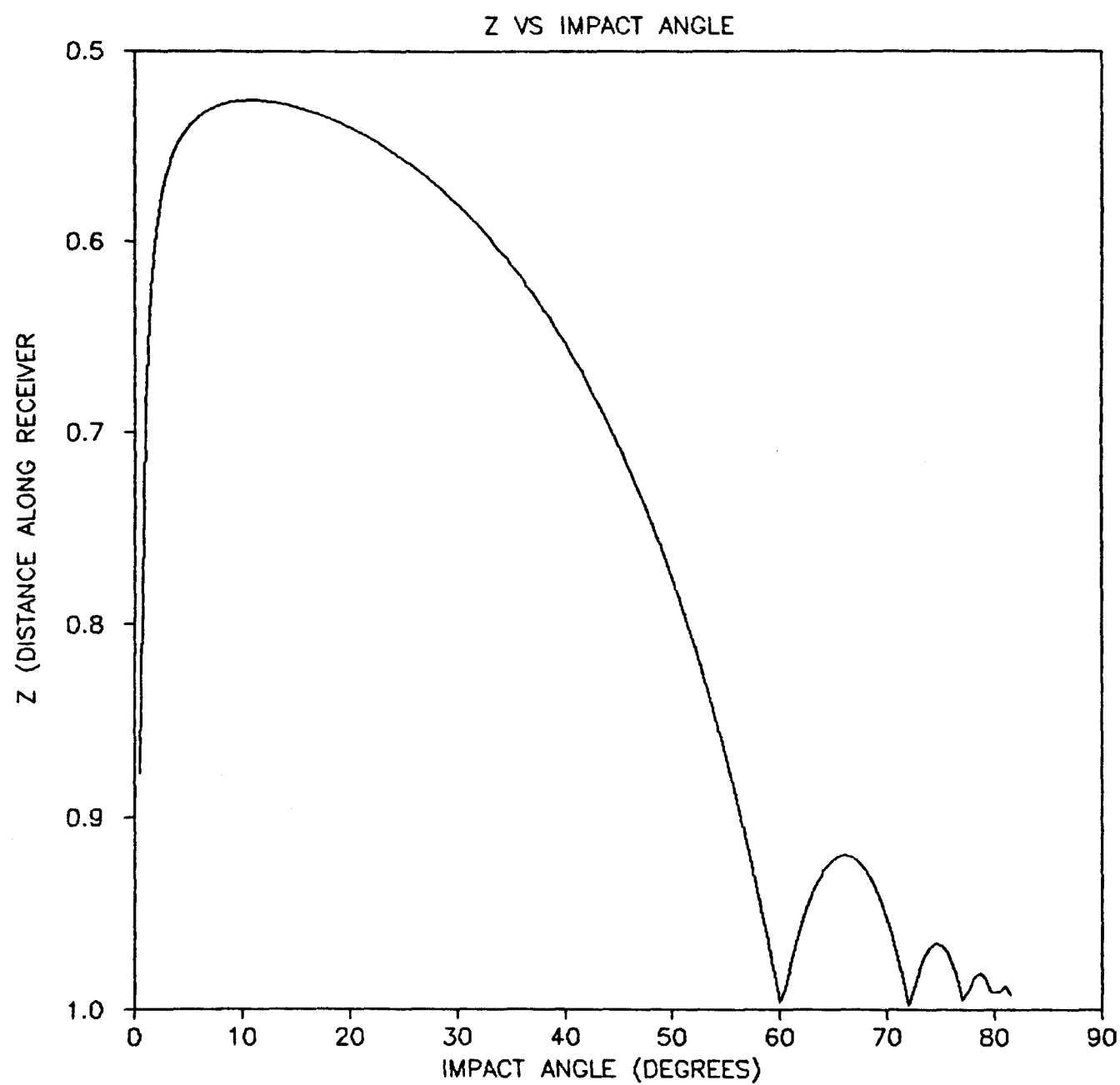


Figure 3.3: Receiver Reception Point vs Impact Angle

$\theta_P < \pi/12$. This region corresponds to rays with impact angles satisfying $\pi/3 \leq \theta \leq 13\pi/36$. All the energy from rays in this region will be lost, i.e., will spill over the edge of the bowl.

In this example, rays of order three have impact angles in the region $2\pi/5 < \theta < 5\pi/12$. These rays require rim support in the region $0 < \theta_P < \pi/12$. Thus all energy for rays of order three will be lost.

In Figure 3.4 the xyz and $\hat{x}\hat{y}\hat{z}$ coordinate systems are related via a rotation through the angle I about the y axis. If we employ spherical coordinates in each system, we obtain the relationship

$$\begin{pmatrix} \sin \theta \cos \phi \\ \sin \theta \sin \phi \\ \cos \theta \end{pmatrix} = \begin{pmatrix} \cos I & 0 & -\sin I \\ 0 & 1 & 0 \\ \sin I & 0 & \cos I \end{pmatrix} \begin{pmatrix} \sin \hat{\theta} \cos \hat{\phi} \\ \sin \hat{\theta} \sin \hat{\phi} \\ \cos \hat{\theta} \end{pmatrix}. \quad (3.13)$$

This yields the set of equations

$$\begin{cases} \sin \theta \cos \phi = \cos I \sin \hat{\theta} \cos \hat{\phi} - \sin I \cos \hat{\theta}, \\ \sin \theta \sin \phi = \sin \hat{\theta} \sin \hat{\phi} \\ \cos \theta = \sin I \sin \hat{\theta} \cos \hat{\phi} + \cos I \cos \hat{\theta}. \end{cases} \quad (3.14)$$

Referring to Figure 3.5, and using the relations in Eq. 3.14, we find that the values, $\hat{\phi}_n$, where the circle $\theta = \theta_n^\pm$ intersects the rim of the bowl are given by

$$\hat{\phi}_n = \pi \mp \hat{\phi}_n^\pm, \quad (3.15)$$

where,

$$\hat{\phi}_n^\pm = \arccos \left[\frac{\cos I \cos \theta_R - \cos \theta_n^\pm}{\sin I \sin \theta_R} \right]. \quad (3.16)$$

It is convenient to carry out all calculations in the (ϕ, θ) coordinate system. In this system, the θ_n^\mp circles intersect the rim at the pair of angles $\pi \mp \phi_n^\mp$ where

$$\phi_n^\mp = \arctan \left[\frac{\sin \theta_R \sin \hat{\phi}_n^\pm}{\cos I \sin \theta_R \cos \hat{\phi}_n^\pm + \sin I \cos \theta_R} \right]. \quad (3.17)$$

We first consider the case where only rays of orders one and two occur. This occurs when I satisfies the condition

$$\pi/3 < I + \theta_R \leq 2\pi/5. \quad (3.18)$$

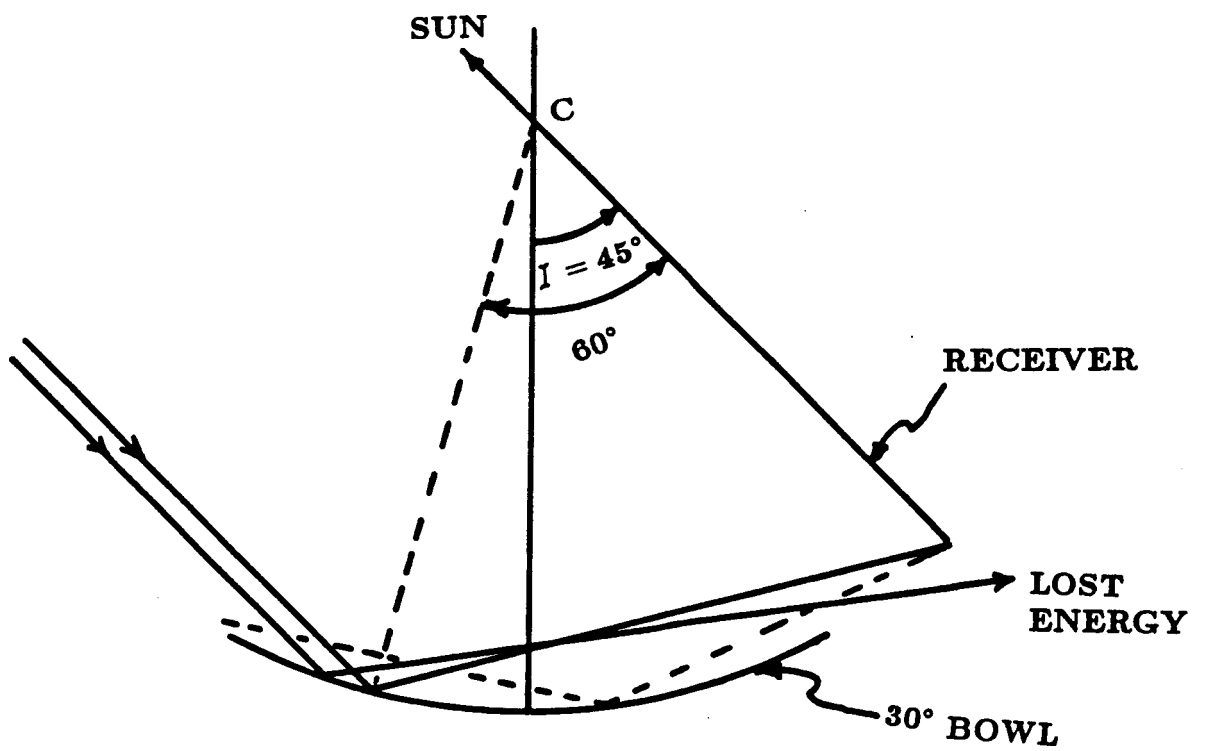


Figure 3.4: Side View of Spillage Geometry

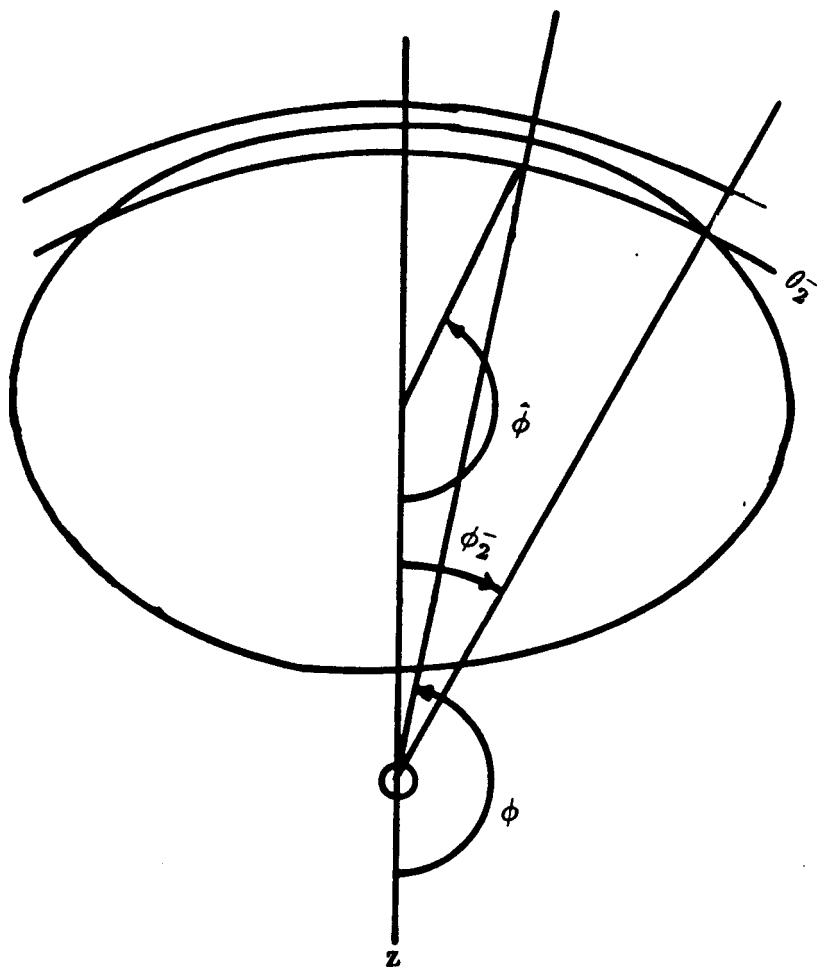


Figure 3.5: Overhead View of Spillage Geometry

Rays that bounce twice occur for $\theta_2^- \leq \theta \leq \theta_u$, where θ_u is the polar angle to the top of the bowl rim. For $\pi - \phi_2^- \leq \phi \leq \pi + \phi_2^+$, we find that $\theta_u(\phi)$ is given by

$$\theta_u(\phi) = \theta_1(\phi) + \theta_2(\phi), \quad (3.19)$$

where,

$$\theta_1(\phi) = \arctan(\cos \phi \tan I), \quad (3.20)$$

and

$$\theta_2(\phi) = \arccos \left[\frac{\cos \theta_R}{\sqrt{\sin^2 I \cos^2 \phi + \cos^2 I}} \right]. \quad (3.21)$$

However, for a given ϕ , the reflected ray will strike the mirror if and only if

$$\theta(\phi) \geq (\pi + \theta_1(\phi) - \theta_2(\phi))/3.$$

This result is obtained by finding the intersection of the ray $\phi = \text{constant}$ with the rim of the bowl nearest the foot of the receiver. The total power lost is computed from the integral

$$P_{\text{LOSS}}(I) = \int_0^{\phi_0} \int_{\pi/3}^{\theta_u} \sin \theta \cos \theta d\theta d\phi \quad (3.22)$$

$$= \int_0^{\phi_0} (\sin^2 \theta_u(\phi) - \sin^2 \pi/3) d\phi, \quad (3.23)$$

where,

$$\theta_u(\phi) = \text{MIN}(\theta_1(\phi) + \theta_2(\phi), (\pi + \theta_1(\phi) - \theta_2(\phi))/3).$$

The details for calculating spillage for larger inclination angles are similar. We first observe that an n -bounce ray is possible only if the relations

$$\theta_n^- < I + \theta_R, \quad (3.24)$$

and,

$$\theta_R - I < \theta_n^+, \quad (3.25)$$

hold. In the case where the relations hold, a range of ϕ values can be calculated to give the set of azimuthal directions of rays of order n . For each ϕ , a range of impact angles, θ , is determined. Spillage occurs for those values of θ for which

$$\theta(\phi) \leq [(n-1)\pi + \theta_1(\phi) - \theta_2(\phi)] / (2n-1). \quad (3.26)$$

The power loss for rays of order n can be determined by integration as in the case illustrated above.

A graph of power vs inclination is shown in Figure 3.6. The top curve gives the total energy into the bowl. The lower curve gives the total power reaching the receiver. The points marked by the \diamond 's are values of total power received on the boiler as computed by the ROSA computer code. In the ROSA calculations, the boiler radius, a , is normalized to represent the radius of the boiler at the Crosbyton Solar Power ADVS site. The graphs are restricted to inclination angles below 60° so that shading will not have to be taken into account in the ray tracing model. Of course, ROSA code easily handles shading. Also, the solar insolation is taken to be unity.

A listing of the computer code that implements the ray tracing method for computing spillage is listed below.

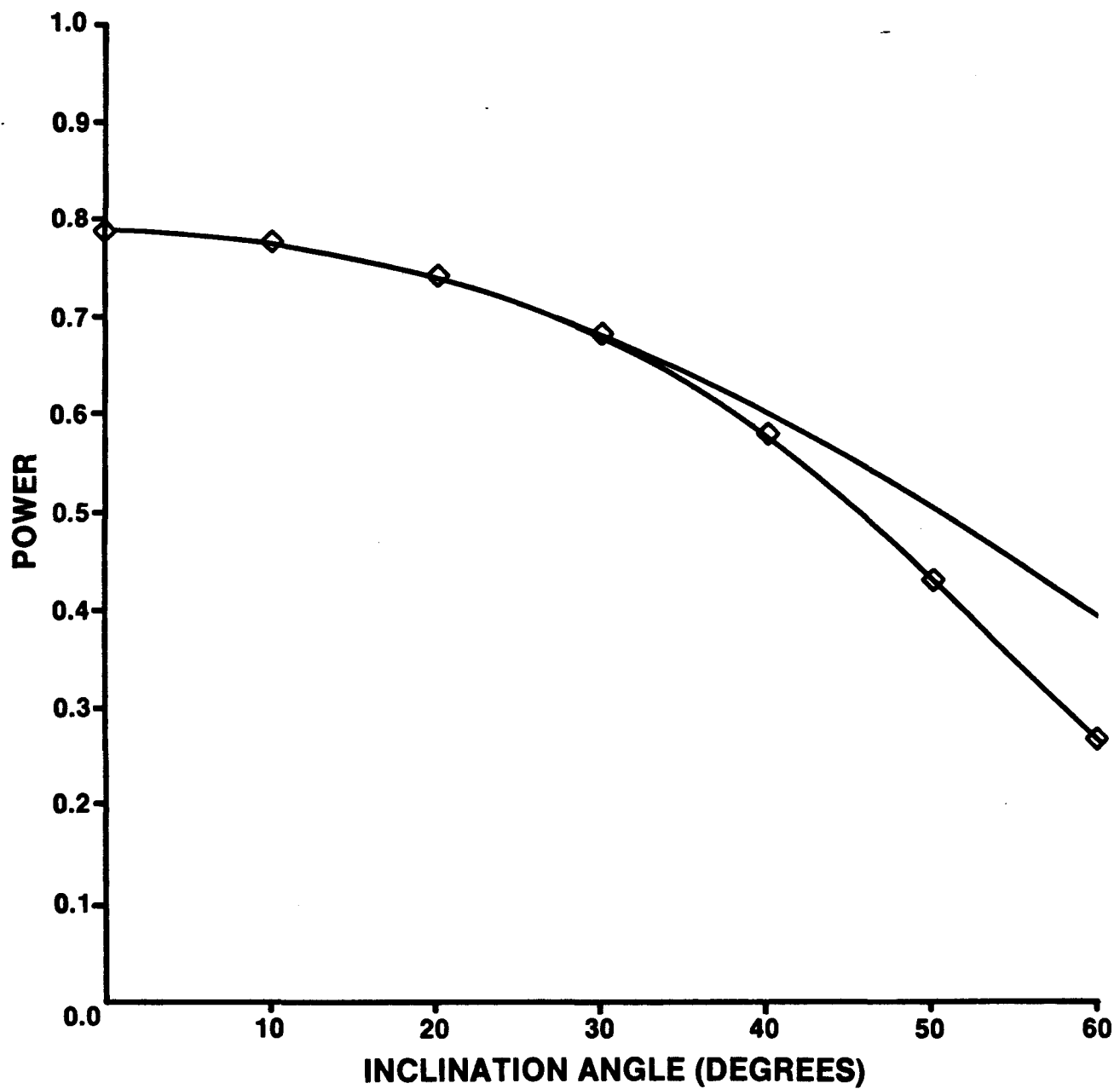


Figure 3.6: Spillage vs Inclination Angle (30° bowl and unit solar insolation).

```

*DECK SPILL
      PROGRAM SPILL
C      PROGRAM TO COMPUTE SPILLAGE LOSSES BY RAY TRACING
C      FOR SHALLOW BOWLS
C      AUTHOR: RONALD M. ANDERSON
C      DATE  : 10/08/86
C
      PI=4.0*ATAN(1.)
      THETAR=PI/6.
      CTHTR=COS(THETAR)
      STHTAR=SIN(THETAR)
      RAD=PI/180.
C      SET UP INCLINATION ANGLE LOOP
      THTARD=THETAR/RAD
      IO=THTARD+1.1
      IE=89.-THTARD
C      COMPUTE TOTAL POWER BY COSINE LAW - NO SPILLAGE
      AREA=PI*STHTAR**2
      DO 05 I=0,IO-1
      P=AREA*COS(I*RAD)
      WRITE(6,*)I,P,P
 5  CONTINUE
      DO 10 I=IO,IE
      DI=REAL(I)*RAD
      CI=COS(DI)
      SI=SIN(DI)
C      FIND LARGEST ORDER OF RAYS
      NM=(DI+THETAR)/(PI-2.0*(DI+THETAR))+1
      DO 20 N=2,NM
      THNP=N*PI/REAL(2*N+1)
      THNM=(N-1)*PI/REAL(2*N-1)
      X=(CI*CTHTAR-COS(THNM))/SI*STHTAR
      IF(X.GT.1.0) THEN
      X=1.0
      ENDIF
      PHIMH=PI-ACOS(X)
      PHIM=ATAN(STHTAR*SIN(PHIMH)/(SI*CTHTAR-CI*STHTAR*COS(PHIMH)))
      NP=(PHIM)/RAD+1.01
      DPHI=(PHIM)/NP

```

```

PHIM=PI-PHIM
DO 30 J=1,NP
    PHI=PHIM+J*DPHI
    CPHI=COS(PHI)
    CTH1=(CTHTAR/SQRT((CI**2+(SI*CPHI)**2)))
    IF(CTH1.GT.1.0)CTH1=1.0
    TH1=ACOS(CTH1)
    TH2=-ATAN(SI*CPHI/CI)
    THL=TH2-TH1
    THUL=((N-1)*PI+THL)/REAL(2*N-1)
    THU=AMIN1(TH1+TH2,THNP,THUL)
    THU=AMAX1(THU,THNM)
    SA=(SIN(THU)**2 - SIN(THNM)**2)
    S=S+SA
30    CONTINUE
    ST=(S-SA)*DPHI+ST
    S=0.0
20    CONTINUE
    P=AREA*COS(I*RAD)
    PS=P-ST
    WRITE(6,*)I,PS,P
    ST=0.0
10    CONTINUE
    STOP
    END

```

Chapter 4

Finite Sun Concentration for a Spherical Mirror

4.1 Introduction

This chapter presents a brief review of the mathematical techniques used in applying the ROSA method for the calculation of optical power profiles for concentrator-receiver systems. A full discussion of the method has been presented previously in [7].

The optical power concentration, C , at a point Q on a receiver is defined as the total normally directed optical power per unit area received at that point. The concentration, C , therefore depends upon the orientation of the element of the receiver surface containing the point Q . In our calculations, C is normalized by dividing by the direct normal insolation incident upon the receiver. The resulting dimensionless quantity becomes a concentration ratio expressed as "number of suns".

The formula which is used in the optical concentration ratio calculations is due to Reichert and Brock [1,2]. It is termed the Ratio of Solid Angles (ROSA) formulation and provides an integral expression for the concentration ratio. This is a general method, applicable to any mirror-receiver combination, with the only complication being the determination of the limits of integration.

The ROSA method deals directly with a finite sun rather than a point sun. The sun's size is expressed in terms of an angular radius, σ . Direct sunlight received at a point is viewed as a collection of rays lying inside

a right circular cone with vertex angle 2σ . The solid angle of this cone is used for normalization purposes. The sun is, to a good approximation, an isotropic radiator (Lambert law radiator), so that the incident flux is uniform in solid angle within the cone [1].

The ROSA formula for the concentration, C , at a receiver point, Q , due to reflection from a mirror surface is given by

$$C(\vec{q}, \hat{b}) = \sum \frac{R^n}{\Omega_{S_n}} \iint_{\Omega_{M_n}} \hat{b} \cdot d\vec{\Omega}, \quad \text{for } \hat{b} \cdot d\vec{\Omega} > 0 \quad (4.1)$$

where,

\vec{q} = the vector locating a field point Q on the receiver with respect to a convenient coordinate system;

\vec{b} = the unit outward normal to the receiver at Q ;

n = the number of times a ray has been reflected on the mirror before striking the receiver at Q ;

$\Omega_{S_n} = 4\pi \sin^2(\sigma_n/2)$, the effective solid angle of the sun as viewed directly from the field point Q ;

σ_n = the effective angular radius of the sun to be used for light which reflects n times in the mirror (for a perfect mirror $\sigma_n = \sigma$);

R = the reflection coefficient of the mirror surface, $0 \leq R \leq 1$;

$d\vec{\Omega}$ = differential solid angle directed toward the apparent position of the sun as viewed in the mirror; i.e., the oriented element of surface area on the unit sphere, with outward normal.

[The “effective” angular radius of the sun, σ_n , is taken to be larger than the true radius in order to account for local slope errors (surface normal pointing errors) of the mirror surface. Statistical analyses (which will not be documented here) show, for example, that $\sigma_1 \approx 2\sigma \approx 0.5^\circ$ (where σ is the actual radius of the solar disk) for mirrors which meet the CSPP specification of 0.06° RMS surface normal error. For such mirrors, $\sigma_n = 2^n \sigma$ [1].

4.2 Geometrical Considerations

In order to evaluate the integral in Equation 4.1, it is convenient to introduce a spherical coordinate system. In this system, the polar axis is chosen to lie along the line CQ and the origin of the system is placed at the field point Q. The integration is to be carried out over Ω_{M_n} . Integration points are specified by an azimuthal angle ω and the zenith angle β , where β is measured from the polar axis as shown in Figure 4.1.

Planes $\omega = \text{constant}$ contain the polar axis and intersect a spherical segment mirror in arcs of great circles. For each ω , the reflection geometry becomes two-dimensional and can be handled in a manner similar to the simplified case discussed in the previous chapter. The problem is more complicated, however, in the case of a finite sun. Instead of two distinct impact angles for reflected rays, there are two families of incident rays that may reflect to a field point. One of these families is illustrated in Figure 4.2

Using the parameters β and ω , one can write the ROSA formula, Equation 4.1 in the form:

$$C(\vec{q}, \hat{b}) = \sum \frac{R^n}{\Omega_{sn}} C_n(\vec{q}, \hat{b}) \quad (4.2)$$

where

$$C_n(\vec{q}, \hat{b}) = \int_{\omega_L}^{\omega_U} \int_{\beta_{L_n}}^{\beta_{U_n}} [(b_x \cos \omega + b_y \sin \omega) \sin^2 \beta + b_z \cos \beta \sin \beta] d\beta d\omega \quad (4.3)$$

The components of \hat{b} are given in a cartesian coordinate system, with origin at Q , using the polar axis as the z -axis. The azimuth ω is measured from the x' -axis. [For a perfectly aligned receiver, the x' -axis can be chosen so that $b_x = \cos \psi$, $b_y = 0$, and $b_z = \sin \psi$.] The integral on β in Eq. 4.3 is elementary and can be performed immediately. The limits β_{U_n} and β_{L_n} are complicated functions of ω , so that the ω -integration is performed numerically.

The basic work of the ROSA code is to determine the limits in the β -integration and then perform the ω -integration. The relevant geometry may be simplified considerably by introducing a *sun cone* with vertex at the center of curvature, C . The family of incidence directions for solar radiation at C forms a right circular cone with vertex at C and angular radius σ . If the rays are extended through C , the second branch of the cone has the

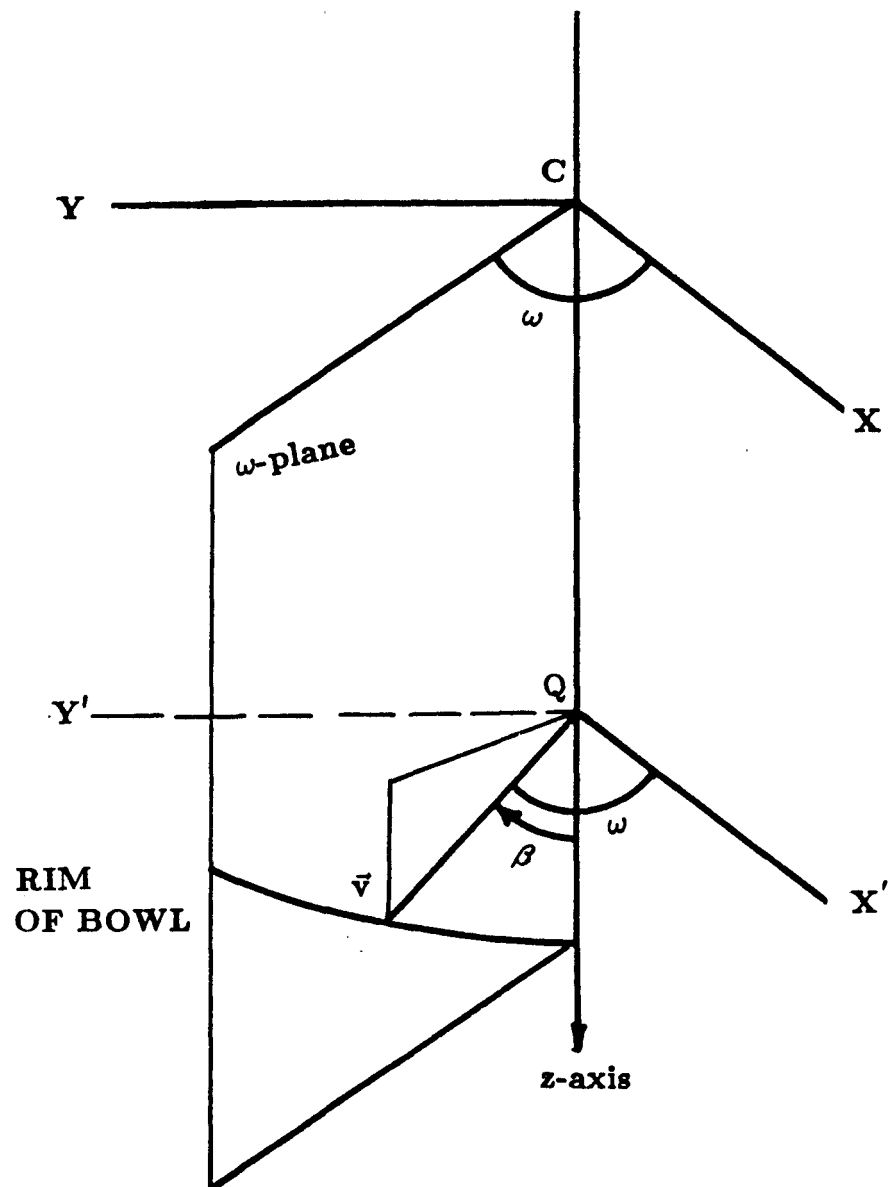


Figure 4.1: Geometry for Integration

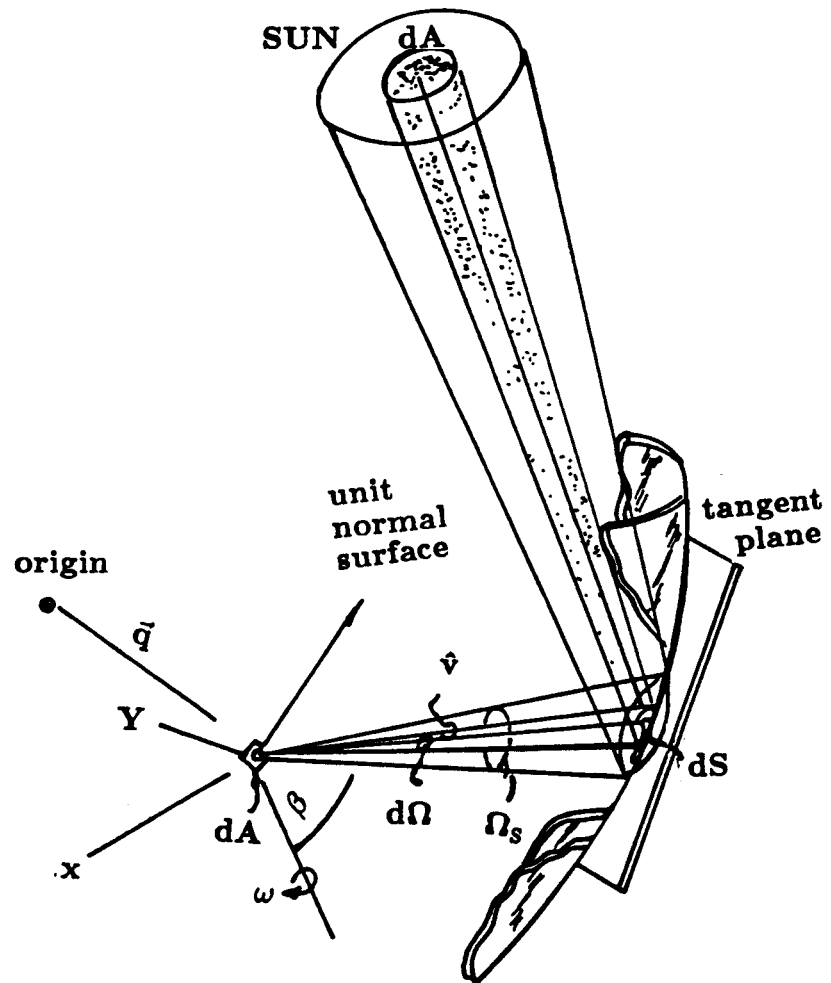


Figure 4.2: Solid Angle Geometry for a Finite Solar Disk

same angular radius, but hangs downward. This inverted branch of the cone is called the *sun cone*. The ranges of integration required by Eq. 4.3 can be determined by considering the intersections of planes of constant ω with the sun cone.

The sun cone defines the set of all possible directions from which direct incident rays can strike the mirror surface. That is, corresponding to every ray that strikes the surface of the mirror, there exists a parallel ray through C that lies in the sun cone. Thus, for each $\omega = \text{constant}$ plane, the set of possible directions of direct rays which can reflect to which the field point Q lies inside the sun cone. In the figure, β is the angle of an incoming reflected ray, as measured from the z -axis, ψ_+ and ψ_- are the extreme values of direct rays in the ω -plane and are measured from the z -axis. For the case in which the field point lies inside the sun cone, every ω -plane intersects the sun cone. For points, Q , outside the sun cone, the ω -plane intersects the sun cone for only certain values of ω .

A detailed consideration of the geometry of the intersection of the ω -plane with the sun cone gives:

$$\psi_{\pm} = \eta \pm \cos^{-1} \left[\frac{\cos \sigma}{\sqrt{(1 - \sin^2 \psi_0 \cos^2 \omega)}} \right] \quad (4.4)$$

where

$$\eta = \tan^{-1} [\tan \psi_0 \cos \omega], \quad \eta \in [-\pi/2, \pi/2]. \quad (4.5)$$

The angle ψ_0 is the central angle of Q measured from the axis of the sun cone. These results are to be used for all cases, with ω restricted so that $\hat{b} \cdot d\vec{\Omega} > 0$.

For each ω , once the range $\psi_-(\omega)$ to $\psi_+(\omega)$ has been determined, then the corresponding values of β can be determined, using

$$\beta = 2n \sin^{-1}(q \sin \beta) - \psi_{\pm} - (n - 1)\pi \quad (4.6)$$

Solution of the above equation yields one or two β -intervals, depending upon the values of ψ_{\pm} . The β limits obtained from Eq. 4.6, restricting ω such that $\hat{b} \cdot d\vec{\Omega} > 0$, may be used to evaluate the integrals in Eq. 4.3.

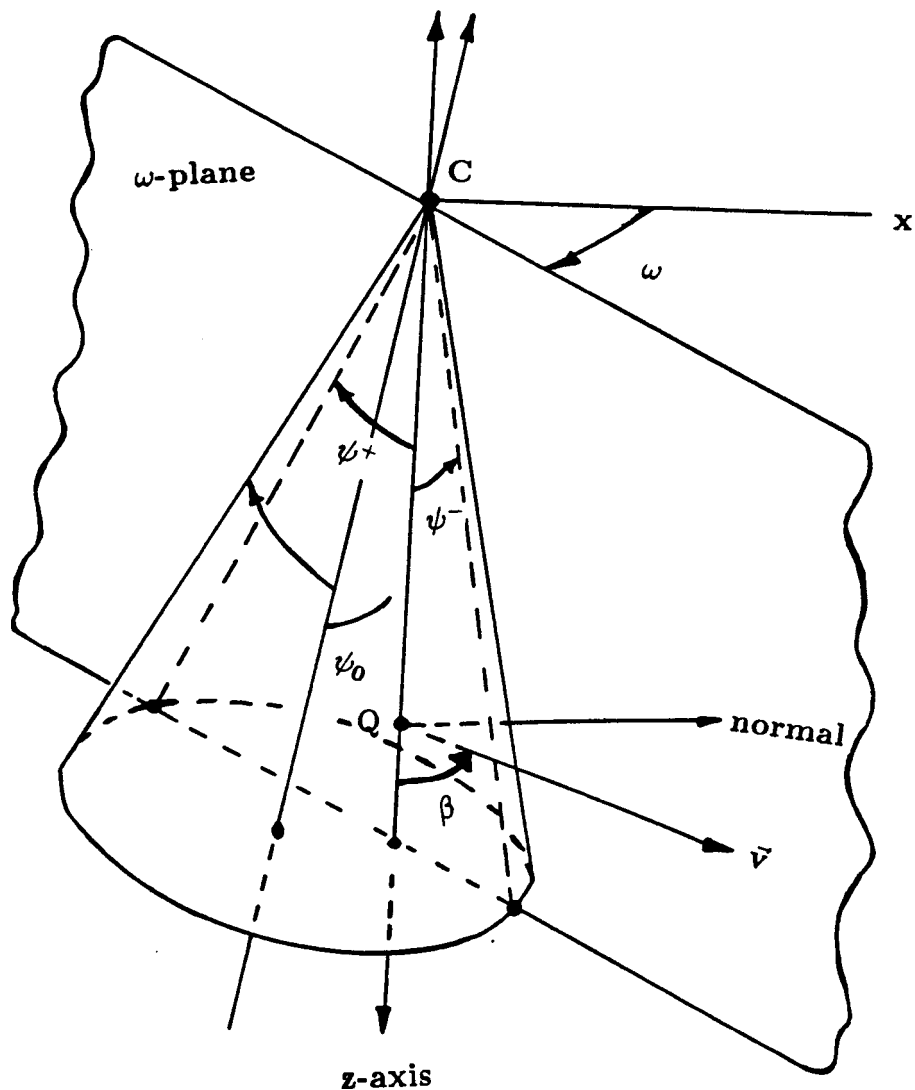


Figure 4.3: The Intersection of a Constant ω -plane with the Sun Cone.

4.3 Shading and Rim Cutoff Effects

For a spherical segment collector, the principal axis of the receiver should be aligned with the sun in order to maximize the amount of energy captured by the receiver. The spherical mirror is stationary. Thus, as the sun passes over the mirror, the effective aperture of the mirror changes, resulting in a loss of power due to either rim cutoff or shading or both. A two-dimensional view of rim-cutoff and shading is shown in Figure 4.4. The total input power is proportional to the cosine of the angle I between the bowl symmetry axis and the direction of the sun. [Rim, not additional fixed aperture penalties.] The cosine effect is accounted for by limiting ranges of integration so that they stop at the bowl rim and/or at the edges of shadows of the rim.

The effect of rim cutoff and shading is easily taken into account in the concentration integral. Since each $\omega = \text{constant}$ plane intersects the bowl in the arc of a great circle, rim cutoff and shading merely decreased the length of the arc. Thus, these effects decrease the length of the β -intervals used in the concentration integrals. The actual calculation of these effects depends on the direction of the sun, on the value of ω , on the location and orientation of the field point on the receiver, and on rim angle of the dish. The detailed derivation of rim angle formulas is carried out in the next chapter.

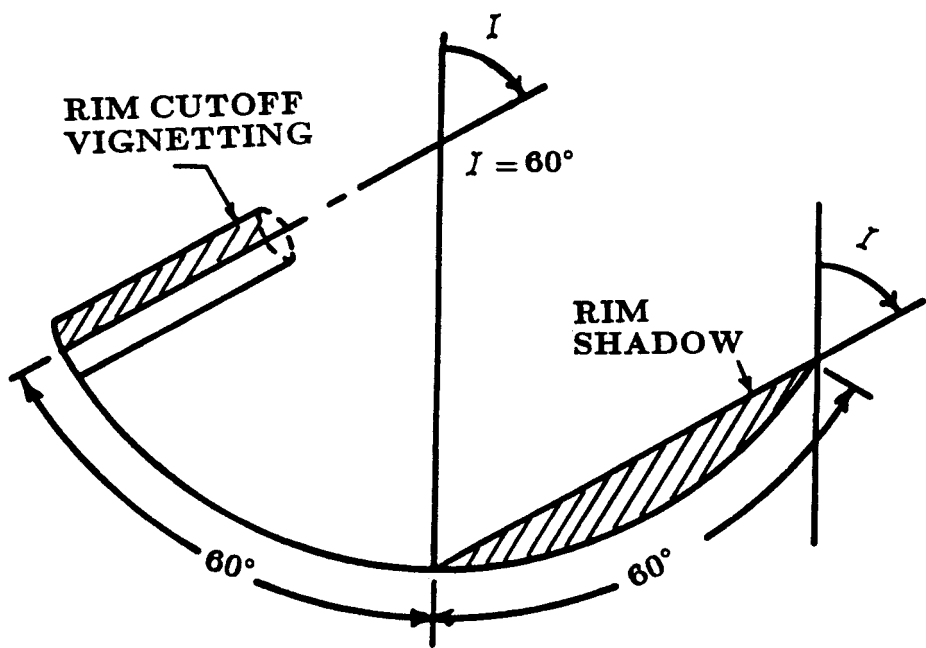


Figure 4.4: Rim Cutoff Effects

Chapter 5

Solar Bowls with an Iris

5.1 Introduction

The original ROSA computer code was implemented for spherical segment solar bowls. This chapter derives the necessary formulas for extending the code to a spherical segment bowl with an iris. The only change required in this code involves the method by which rim angle effects are calculated.

The previous chapter outlined the general method used in the ROSA code for the evaluation of the concentration integral. The calculations employ a local spherical coordinate system with a zenith angle β and azimuthal angle ω . A fixed value of ω defines a plane that intersects the bowl surface in a segment of a great circle. This is illustrated in Figure 5.1. In this figure, Q represents a field point on the receiver and C is the center of symmetry of the bowl. A local $x'y'z'$ -coordinate system is defined with origin at Q , with the z' -axis along the line segment \overline{CQ} and directed downward. ω is the azimuthal angle in this system, measured from the x' -axis, and β is the zenith angle. An xyz -system is obtained by translating the origin of the $x'y'z'$ -system from Q to C .

The plane $\omega=\text{constant}$ intersects the bowl in the arc of a great circle. The extreme points on the arc correspond to the points where the great circle intersects the rim of the bowl. The dish rim angles in the ω -plane are expressed as a front-side rim angle, θ_z^+ , and a back-side rim angle, θ_z^- . Both θ_z^+ and θ_z^- are zeniths measured from the z -axis. These angles are treated as positive angles in the right half of the ω -plane, negative in the left half plane. The values of θ_z^+ and θ_z^- define extreme values for the set of impact

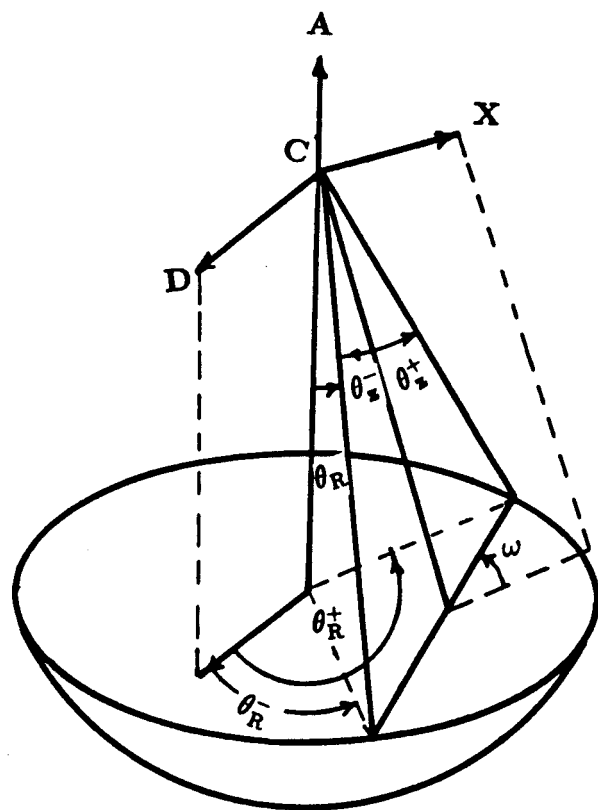


Figure 5.1: Angles Used in Rim-cutoff Calculations

angles for rays that enter the bowl in the ω -plane. In the evaluation of the concentration integral, ω ranges over $[0, 2\pi]$, and only rays which strike the receiver in the right half of the ω plane are considered. This gives the restriction on the impact angle, θ ,

$$\text{MAX} [0, \theta_z^-] \leq \theta \leq \theta_z^+. \quad (5.1)$$

In addition, rim shading occurs for $\theta_z^+ > \pi/2$. Details of shading are discussed in [7].

5.2 Determination of Rim-cutoff Angles for a Spherical Segment Bowl

The values of the rim-cutoff angles θ_z^+ and θ_z^- depend upon the direction of the sun, the location and orientation of the field point Q, on the value of ω , and on the shape of dish rim.

The sun is located in a *SEV* coordinate system (south, east, vertical) centered at C. The location of the sun is specified by a azimuth angle, \mathcal{A} , measured from the south axis and an elevation angle, \mathcal{E} (See Figure 5.2).

A collector fixed coordinate system, (*DMA*-system) with origin at C is used to describe the bowl. The rim itself is described by spherical coordinates (ϕ_R, θ_R) , where θ_R is the rim angle of the bowl and is measured from the axis of symmetry of the bowl (the negative *D*-axis). The *SEV* and *DMA* systems are related by a tilt angle, γ and a dip angle ϕ_d (See Figure 5.3).

The *xyz* and *DMA* coordinate systems are related via a rotation matrix (See Figure 5.1). The relationship can be written in the form

$$\begin{pmatrix} \cos \phi \sin \theta \\ \sin \phi \sin \theta \\ \cos \theta \end{pmatrix} = \begin{pmatrix} R_{11} & R_{12} & R_{13} \\ R_{21} & R_{22} & R_{23} \\ R_{31} & R_{32} & R_{33} \end{pmatrix} \begin{pmatrix} \cos \omega \sin \theta_z \\ \sin \omega \sin \theta_z \\ \cos \theta_z \end{pmatrix}, \quad (5.2)$$

where (ϕ, θ) are azimuthal and zenith angles in the *DMA*-system and (ω, θ_z) are azimuthal and zenith angles in the *xyz*-system. Equating components in this equation yields the system of equations

$$\cos \phi \sin \theta = (R_{11} \cos \omega + R_{12} \sin \omega) \sin \theta_z + R_{13} \cos \theta_z, \quad (5.3)$$

$$\sin \phi \sin \theta = (R_{21} \cos \omega + R_{22} \sin \omega) \sin \theta_z + R_{23} \cos \theta_z, \quad (5.4)$$

$$\cos \theta = (R_{31} \cos \omega + R_{32} \sin \omega) \sin \theta_z + R_{33} \cos \theta_z. \quad (5.5)$$

For a spherical segment bowl, the rim is defined by $\theta = \pi - \theta_R$. Substituting this value into Equation 5.5, we find that

$$\theta_z^\pm = \theta_A(\omega) \pm \theta_B(\omega), \quad (5.6)$$

where,

$$\theta_A(\omega) = \text{ATAN2}(-[R_{31} \cos \omega + R_{32} \sin \omega], -R_{33}), \quad (5.7)$$

and,

$$\theta_B(\omega) = \arccos \left[\frac{\cos \theta_R}{\sqrt{(R_{31} \cos \omega + R_{32} \sin \omega)^2 + R_{33}^2}} \right]. \quad (5.8)$$

5.3 Extension to Bowl with Iris

In order to take advantage of the fact that an iris tracks the sun, it is convenient to introduce a $D'M'A$ coordinate system, centered at C , obtained by a rotation about the A -axis. The D' axis is chosen so that it lies in the plane determined by the A -axis and the vector \mathbf{e}_s that points from C to the center of the sun. If the sun is directly above the A -axis, we take D' to coincide with D . This coordinate system is shown in Figure 5.4.

The location of the D' -axis is calculated as follows. The unit vector \mathbf{e}_s is described in the SEV -system in component form as (See Figure 5.2)

$$\mathbf{e}_s = \begin{pmatrix} \cos \alpha \cos \varepsilon \\ \sin \alpha \cos \varepsilon \\ \sin \varepsilon \end{pmatrix}. \quad (5.9)$$

Referring to Figure 5.3 we find that coordinates in the SEV and DMA coordinate systems are related by the rotation matrix

$$\begin{pmatrix} D \\ M \\ A \end{pmatrix} = \begin{pmatrix} \cos \gamma \cos \phi_d & \cos \gamma \sin \phi_d & -\sin \gamma \\ -\sin \phi_d & \cos \phi_d & 0 \\ \sin \gamma \cos \phi_d & \sin \gamma \sin \phi_d & \cos \gamma \end{pmatrix} \begin{pmatrix} S \\ E \\ V \end{pmatrix}. \quad (5.10)$$

Substitution of the representation of \mathbf{e}_s in the SEV -system into this formula yields the representation for \mathbf{e}_s in the DMA -system as

$$D = \cos \gamma \cos \varepsilon \cos(\alpha - \phi_d) - \sin \gamma \sin \varepsilon \quad (5.11)$$

$$M = \cos \varepsilon \sin(\alpha - \phi_d) \quad (5.12)$$

$$A = \sin \gamma \cos \varepsilon \cos(\alpha - \phi_d) + \sin \varepsilon \cos \gamma \quad (5.13)$$

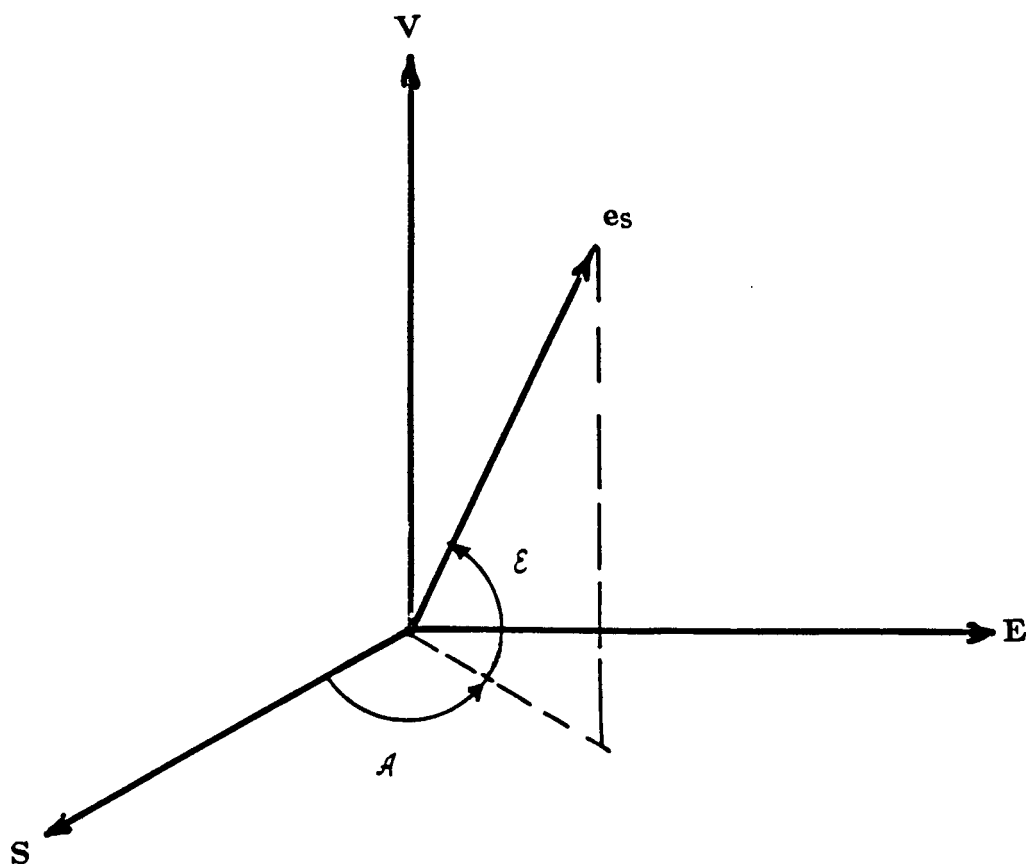


Figure 5.2: Location of the Sun in the *SEV*-system

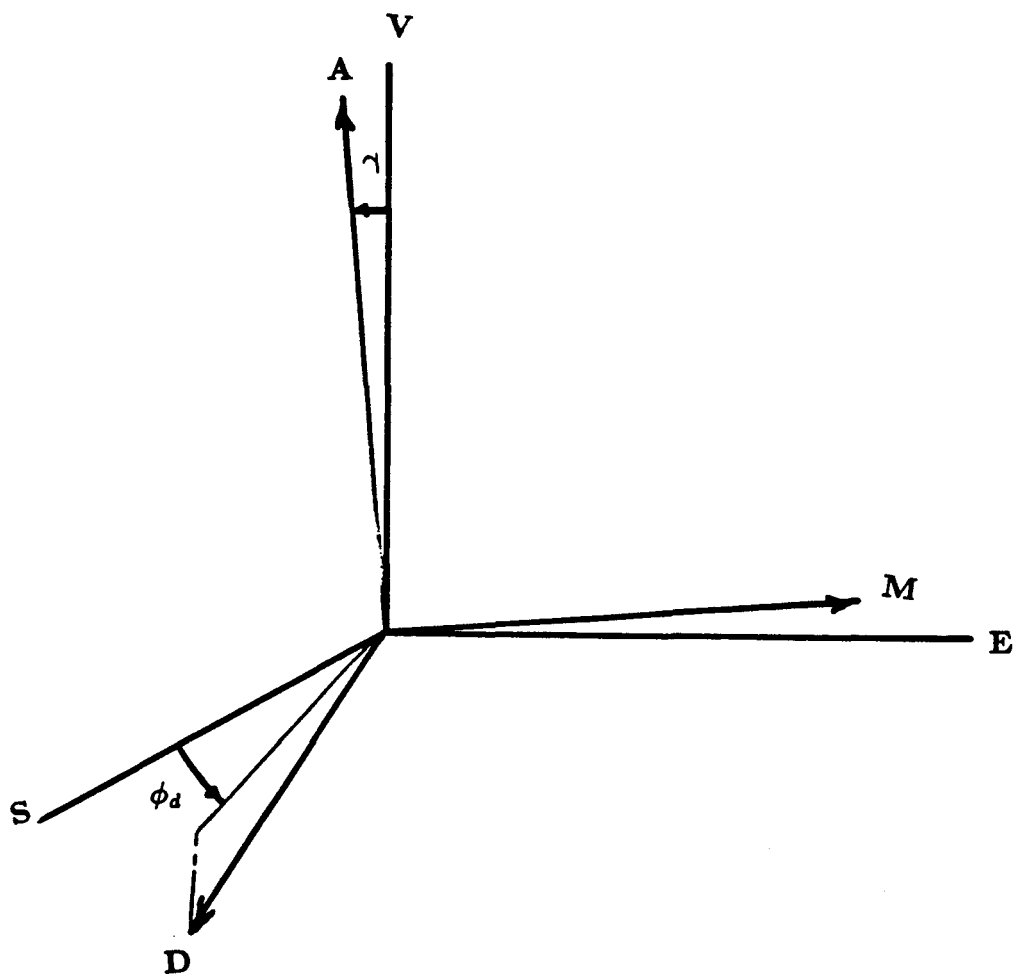


Figure 5.3: The *SEV* and *DMA* Coordinate Systems

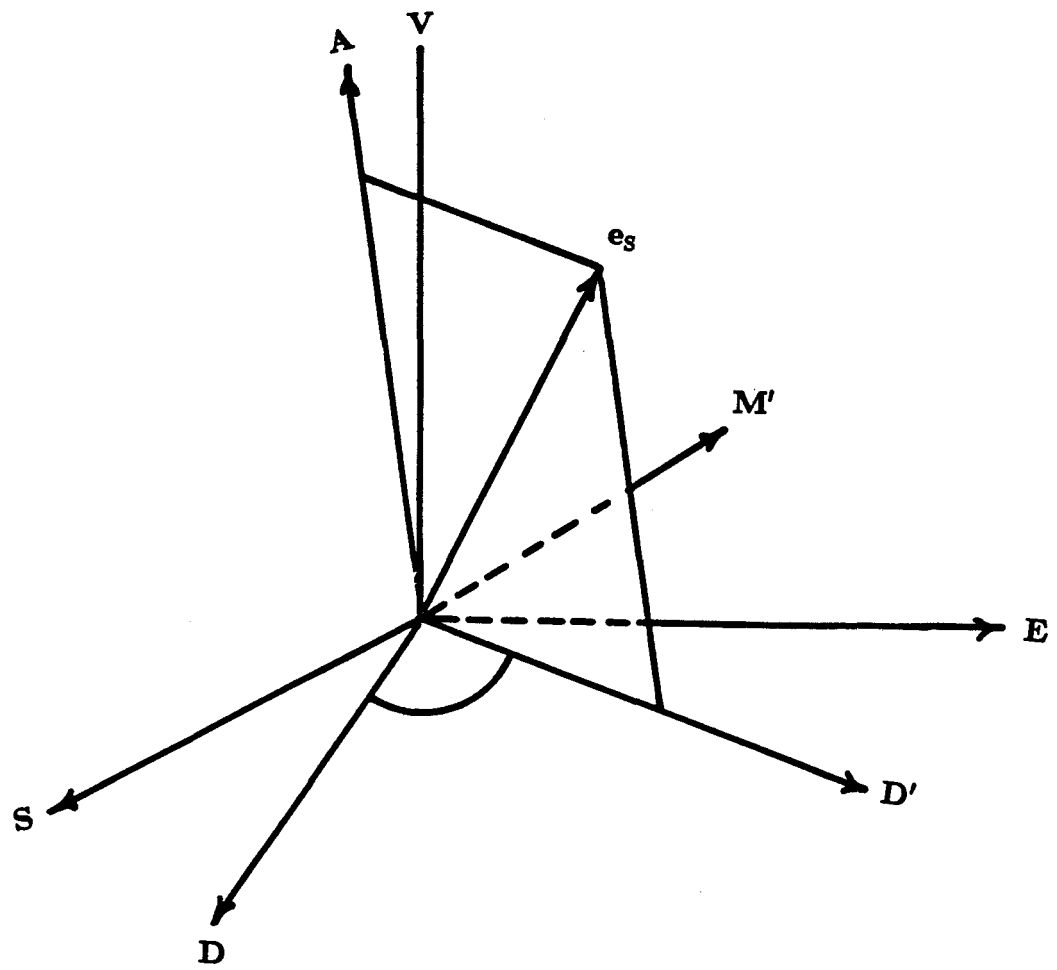


Figure 5.4: Location of the $D'M'A$ Coordinate System

We choose the D' -axis so that it coincides with the projection of \mathbf{e}_s in the DM -plane. This yields a rotation angle, $\phi_{d'}$, about the A -axis given by

$$\phi_{d'} = \text{ATAN2}(M, D), \quad (5.14)$$

where M and D are given by Equations 5.12 and 5.11, respectively. Coordinates in the $D'M'A$ -system are calculated from coordinates in the DMA -system via the rotation matrix

$$\begin{pmatrix} D' \\ M' \\ A \end{pmatrix} = \begin{pmatrix} \cos \phi_{d'} & \sin \phi_{d'} & 0 \\ -\sin \phi_{d'} & \cos \phi_{d'} & 0 \\ 0 & 0 & 1 \end{pmatrix} \begin{pmatrix} D \\ M \\ A \end{pmatrix}. \quad (5.15)$$

Equations 5.3-5.5 become (in the $D'M'A$ -system)

$$\cos \phi \sin \theta = (S_{11} \cos \omega + S_{12} \sin \omega) \sin \theta_z + S_{13} \cos \theta_z, \quad (5.16)$$

$$\sin \phi \sin \theta = (S_{21} \cos \omega + S_{22} \sin \omega) \sin \theta_z + S_{23} \cos \theta_z, \quad (5.17)$$

$$\cos \theta = (R_{31} \cos \omega + R_{32} \sin \omega) \sin \theta_z + R_{33} \cos \theta_z, \quad (5.18)$$

where,

$$\begin{cases} S_{11} = R_{11} \cos \phi_{d'} + R_{21} \sin \phi_{d'}, \\ S_{12} = R_{12} \cos \phi_{d'} + R_{22} \sin \phi_{d'}, \\ S_{13} = R_{13} \cos \phi_{d'} + R_{23} \sin \phi_{d'}, \\ S_{21} = -R_{11} \sin \phi_{d'} + R_{12} \cos \phi_{d'}, \\ S_{22} = -R_{12} \sin \phi_{d'} + R_{22} \cos \phi_{d'}, \\ S_{23} = -R_{13} \sin \phi_{d'} + R_{23} \cos \phi_{d'}, \end{cases} \quad (5.19)$$

and the R'_{ij} 's are the matrix elements appearing in Equation 5.2.

We assume that the iris is symmetric with respect to the $D'A$ plane. Then, the iris is centered on the negative D' -axis.

5.4 An Example

We consider the case of a tracking iris of the form (See Figure 2.3)

$$\begin{cases} \pi - \phi_0 \leq \phi \leq \pi + \phi_0, \\ \theta_R \leq \pi - \theta \leq \theta_L. \end{cases}, \quad (5.20)$$

where ϕ is the azimuthal angle measured from the positive D' -axis and θ is the zenith angle measured from the A -axis.

The solution is carried out in two steps. We find the solutions $\theta_z^\pm(\theta_R)$ for the intersection of the ω -plane with a spherical segment bowl with rim angle θ_R , and also find the solutions $\theta_z^\pm(\theta_I)$ corresponding to a bowl with rim angle θ_I . These solutions are calculated using Equations 5.6-5.8.

For each θ_z , we find the corresponding azimuthal angle, ϕ . These solutions are found using Equations 5.16 and 5.17. Since $0 \leq \theta \leq \pi$, we have $\sin \theta \geq 0$. Therefore, the corresponding azimuthal angle ϕ is calculated as

$$\tan \phi = \frac{(S_{21} \cos \omega + S_{22} \sin \omega) \sin \theta_z + S_{23} \cos \theta_z}{(S_{11} \cos \omega + S_{12} \sin \omega) \sin \theta_z + S_{13} \cos \theta_z}. \quad (5.21)$$

Several cases arise. They are illustrated in Figure 5.5.

1. If $|\phi_z^+(\theta_I)| > \pi - \phi_0$ then $\theta_z^+ = \theta_I$.
(A-3, B-4, B-5, and C-3 in Figure 5.5.)
2. If $|\phi_z^+(\theta_I)| \leq \pi - \phi_0$ and $|\phi_z^+(\theta_R)| \leq \pi - \phi_0$, then $\theta_z^+ = \theta_R$.
(A-1, B-1, and C-1 in Figure 5.5.)
3. If $|\phi_z^+(\theta_I)| \leq \pi - \phi_0$ and $|\phi_z^+(\theta_R)| > \pi - \phi_0$ or $\phi_z^+(\theta_R)$ is not defined (ω -plane does not intersect the spherical segment bowl), then θ_z^+ is computed using Equations 5.16 and 5.17. This gives

$$\tan \theta_z^+ = \frac{S_{23} \cos \phi - S_{13} \sin \phi}{(S_{11} \cos \omega + S_{12} \sin \omega) \sin \phi - (S_{21} \cos \omega + S_{22} \sin \omega) \cos \phi},$$

where

$$\begin{aligned} \phi &= \pi - \phi_0 & \text{if } \phi_z^+ > 0, \\ \phi &= \pi + \phi_0 & \text{if } \phi_z^+ < 0. \end{aligned}$$

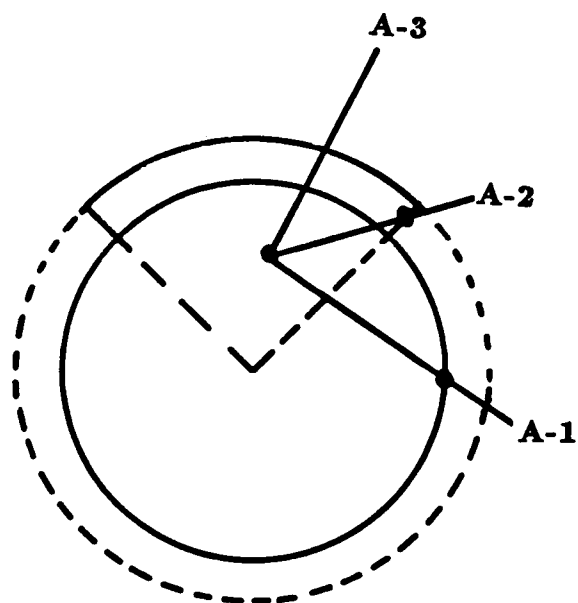
(A-2, B-2, B-3, and C-2 in Figure 5.5.)

4. $|\phi_z^+(\theta_I)|$ is not defined. In this case no bowl support is available for the incoming rays and we set $\theta_z^+ = 0$.
(C-4 in Figure 5.5.)

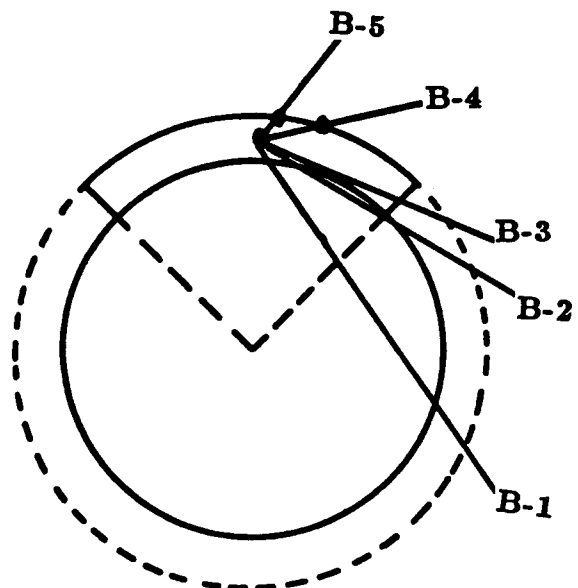
Calculation of θ_z^- is much simpler. It is given by

$$\theta_z^- = \text{MAX} [0, \theta_I^-].$$

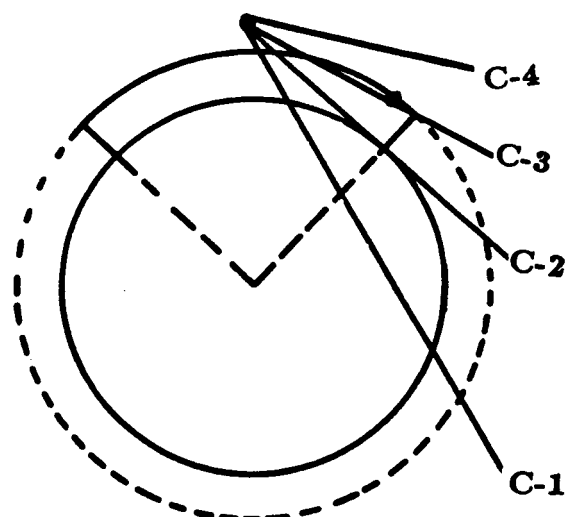
These formulas have been incorporated into the **ROSA** computer code to form the **ROSAIRIS** computer code. Results for the example discussed in this section are presented in the next chapter.



A. Receiver Inside Bowl



B. Receiver Over Iris



C. Receiver Outside Bowl and Iris

Figure 5.5: Intersection of the ω -plane with the Rim

Chapter 6

Optical Concentration Results

This chapter presents several sets of sample output comparing a solar bowl without iris and a solar bowl with iris. In presenting the results, we assume a reflection coefficient of 1 and a perfect reflecting surface. The receiver is chosen to be a right circular cone with angular radius equal to that of the sun cone. Other samples are readily generated by altering the input data for the program.

The first plot compares total power entering the bowl with total power captured by the receiver. The solid curve represents energy entering the bowl and the Δ values represent total power on the receiver. These later values are calculated using ROSAIRIS. Note that spillage occurs for inclination angles larger than 45° .

The remaining plots show solar profiles as a function of distance along the receiver axis. Each plot contains two graphs, one corresponding to a spherical segment bowl, and the second corresponding to the spherical segment bowl with iris. The spherical segment bowl has a rim angle of $\theta_R = 30^\circ$. The iris has rim angle $\theta_I = 45^\circ$ and angular width of $2\phi_0 = 90^\circ$. Plots are presented with the inclination angle of the sun varying from $I = 0^\circ$ to $I = 80^\circ$ in 10° steps.

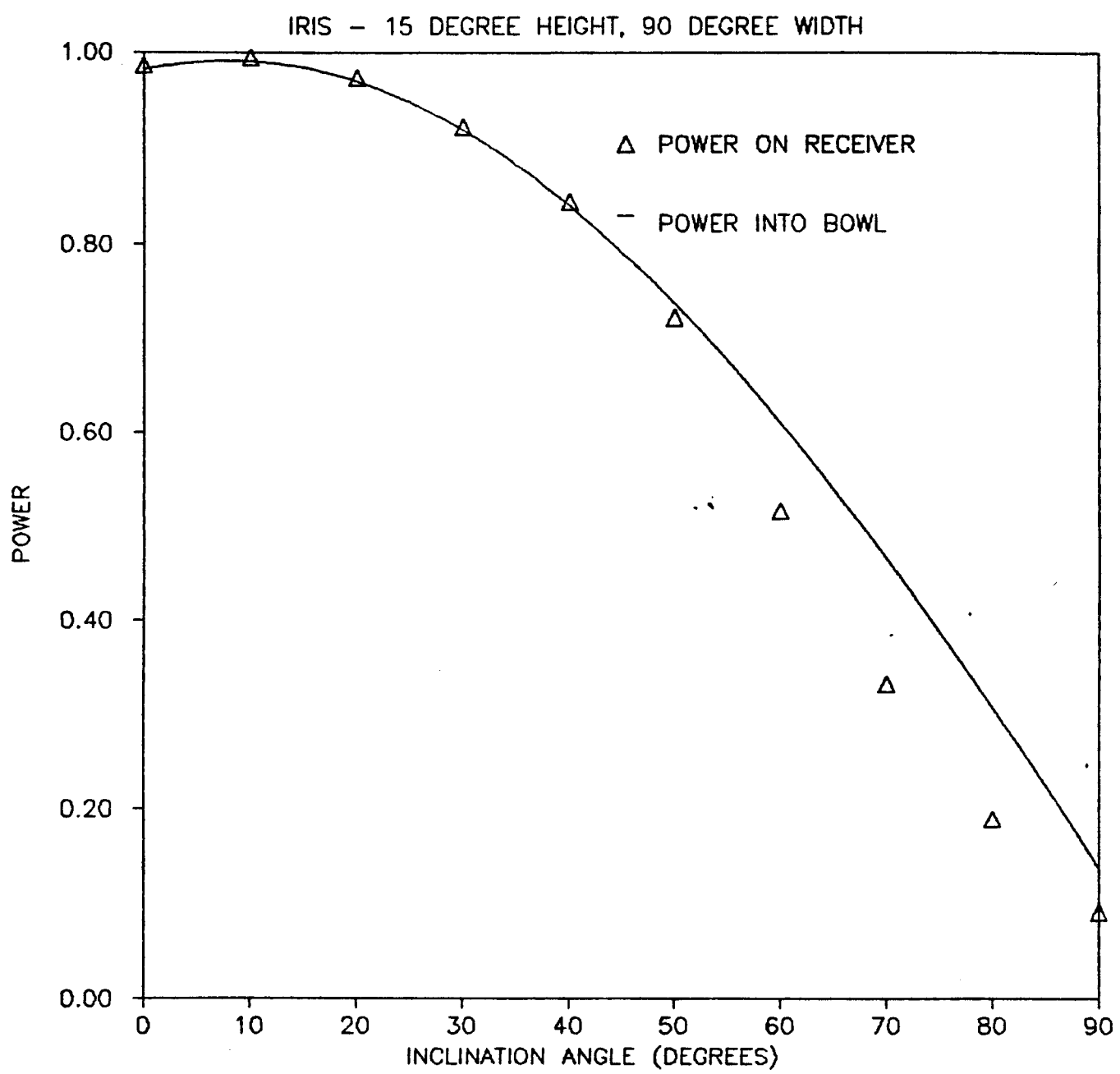
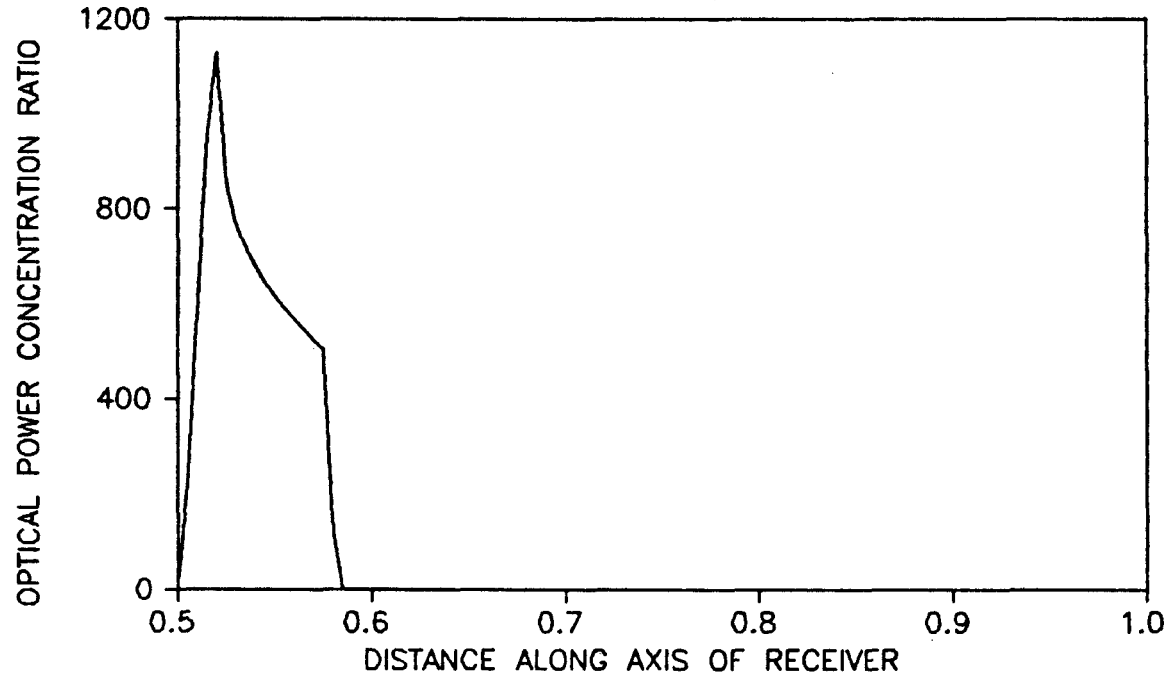


Figure 6.1: Comparison of Input Energy and Captured Energy

SPHERICAL SEGMENT BOWL



SPHERICAL SEGMENT BOWL WITH IRIS

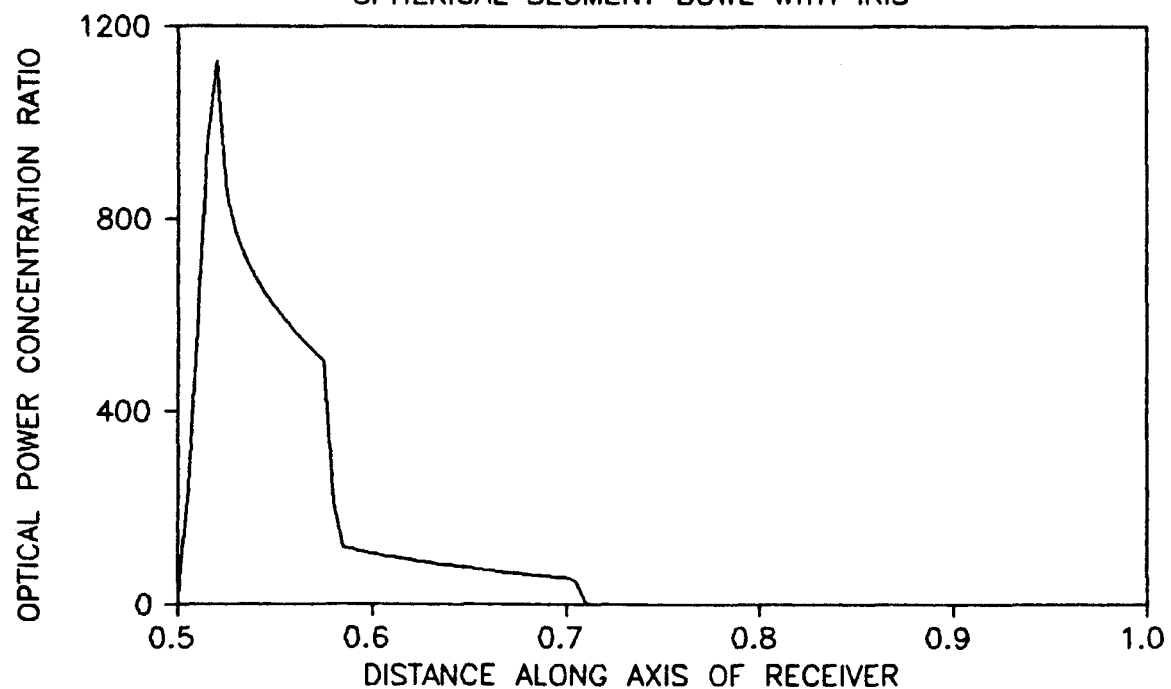
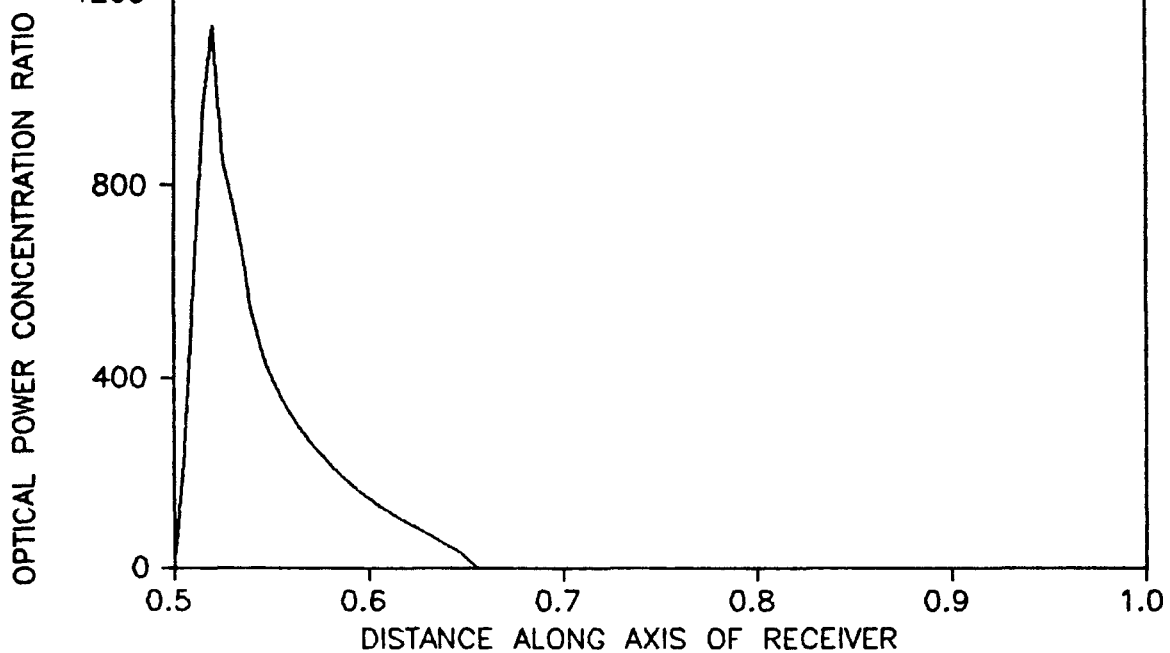


Figure 6.2: Optical Power Concentration for $I = 00^\circ$ and $\theta_R = 30^\circ$, $\theta_I = 45^\circ$, $\phi_0 = 45^\circ$

SPHERICAL SEGMENT BOWL



SPHERICAL SEGMENT BOWL WITH IRIS

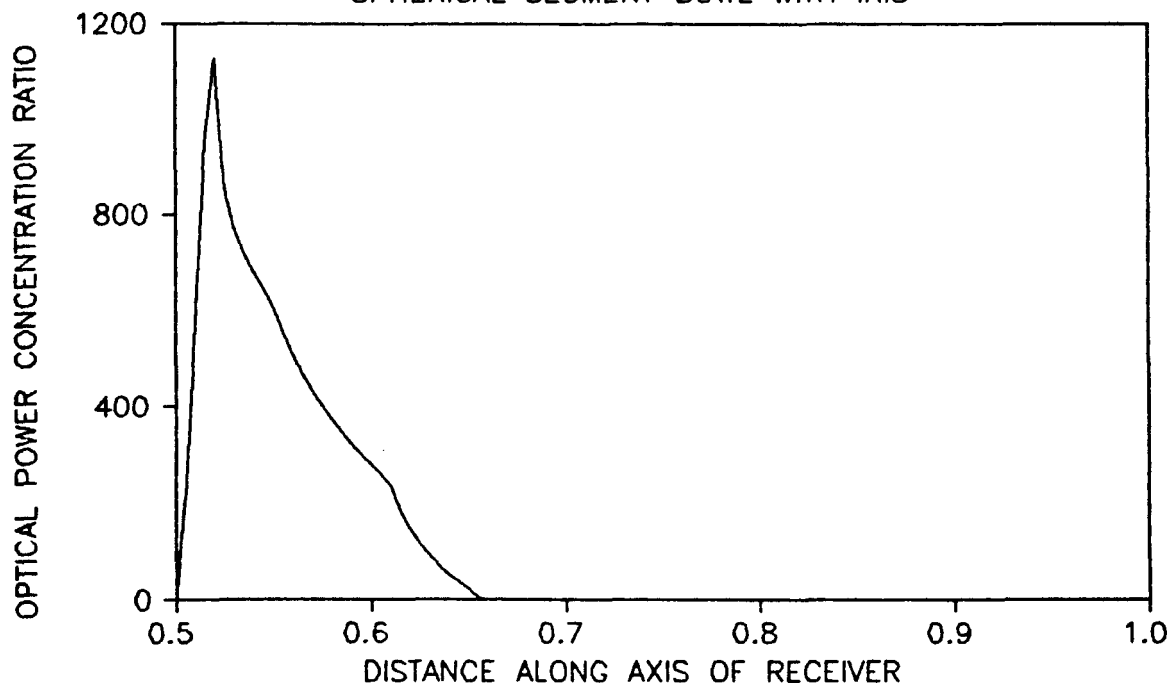
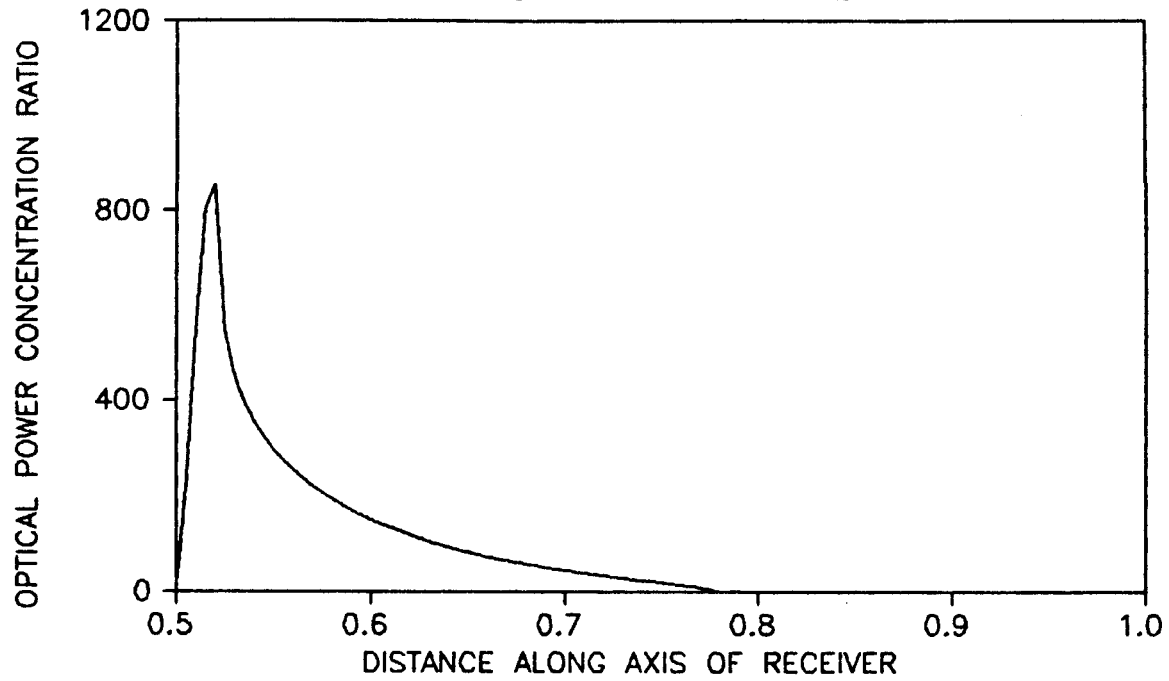


Figure 6.3: Optical Power Concentration for $I = 10^\circ$ and $\theta_R = 30^\circ$, $\theta_I = 45^\circ$, $\phi_0 = 45^\circ$

SPHERICAL SEGMENT BOWL



SPHERICAL SEGMENT BOWL WITH IRIS

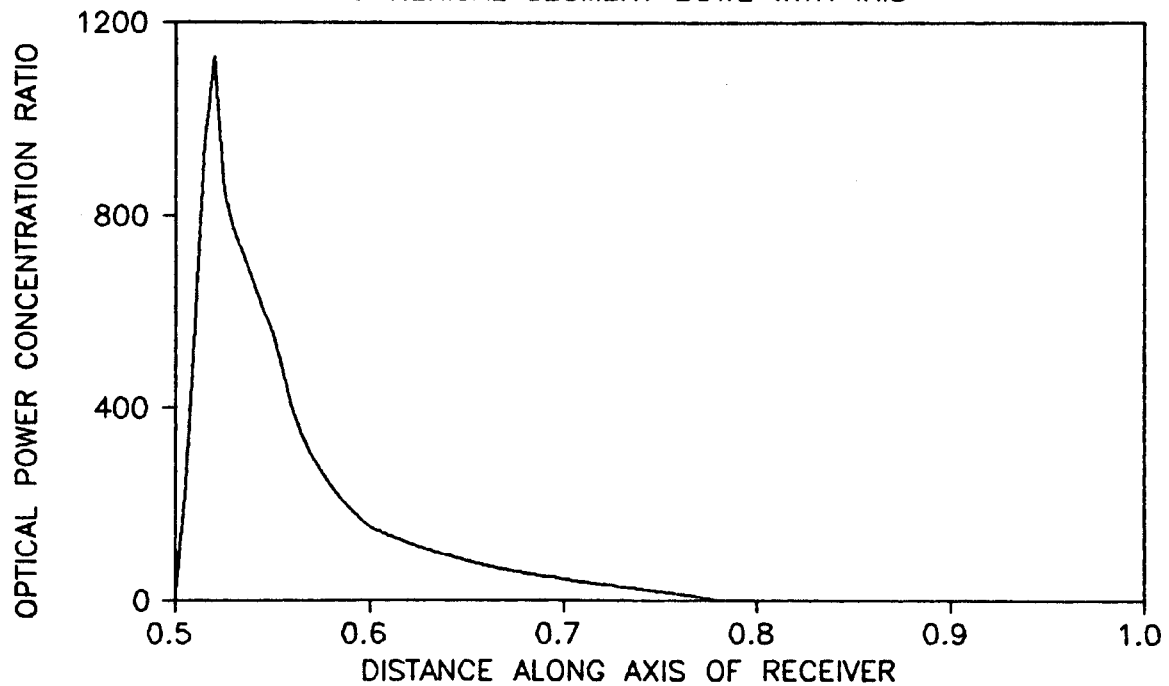
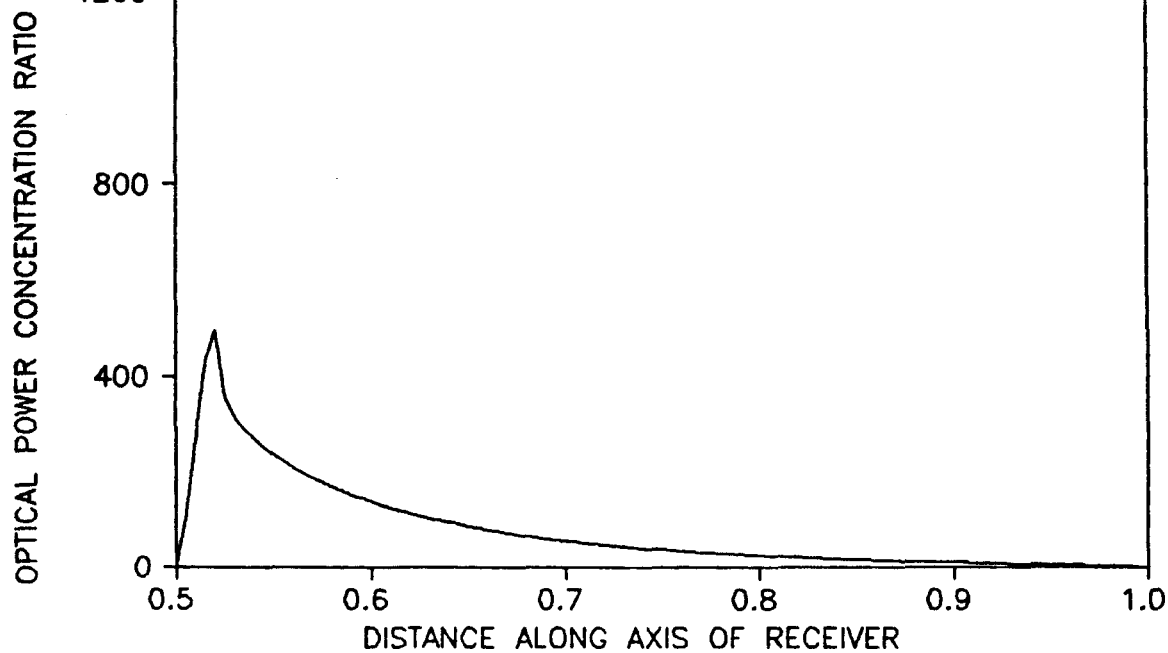


Figure 6.4: Optical Power Concentration for $I = 20^\circ$ and $\theta_R = 30^\circ$, $\theta_I = 45^\circ$, $\phi_0 = 45^\circ$

SPHERICAL SEGMENT BOWL



SPHERICAL SEGMENT BOWL WITH IRIS

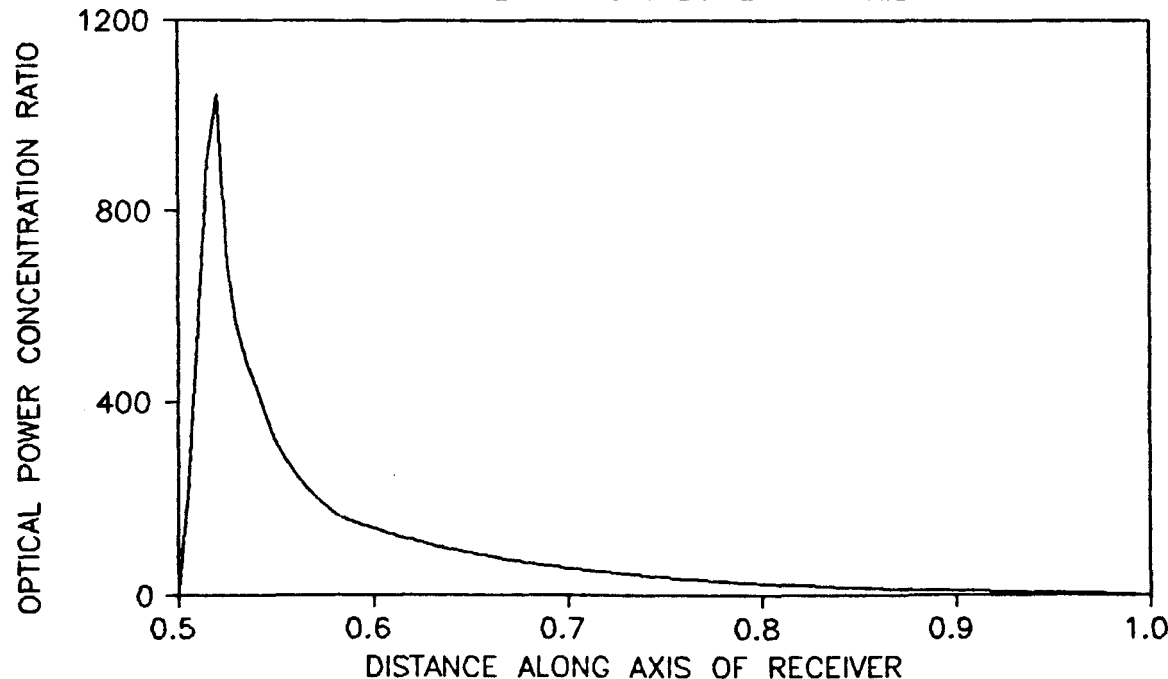
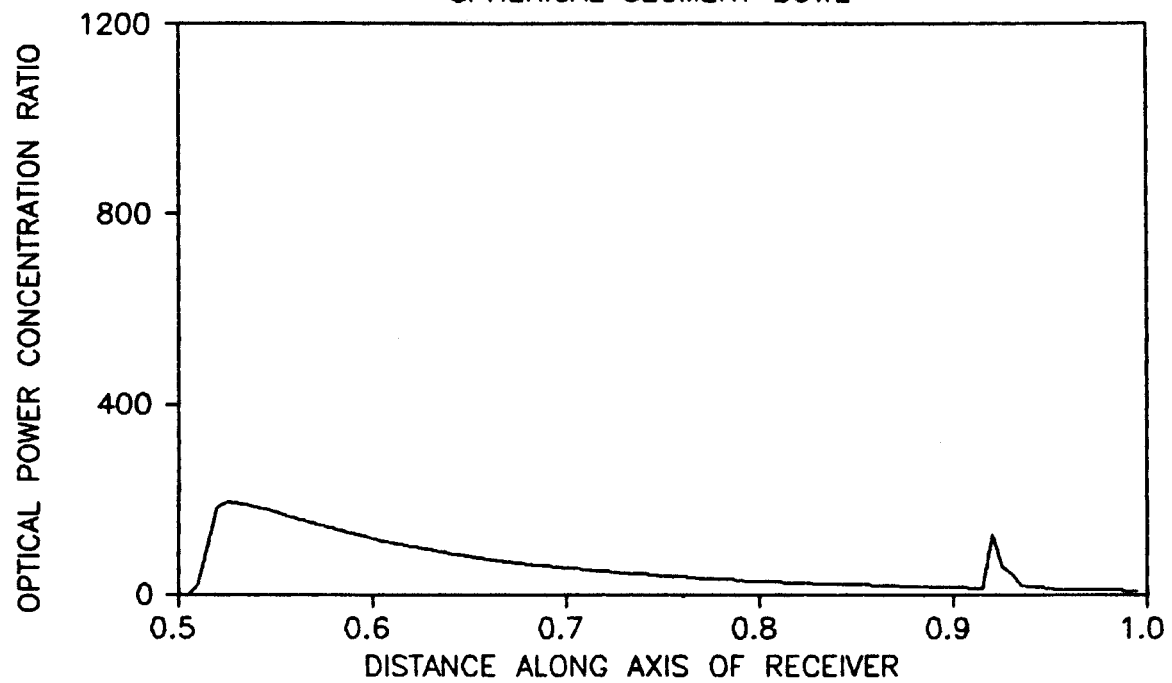


Figure 6.5: Optical Power Concentration for $I = 30^\circ$ and $\theta_R = 30^\circ$, $\theta_I = 45^\circ$, $\phi_0 = 45^\circ$

SPHERICAL SEGMENT BOWL



SPHERICAL SEGMENT BOWL WITH IRIS

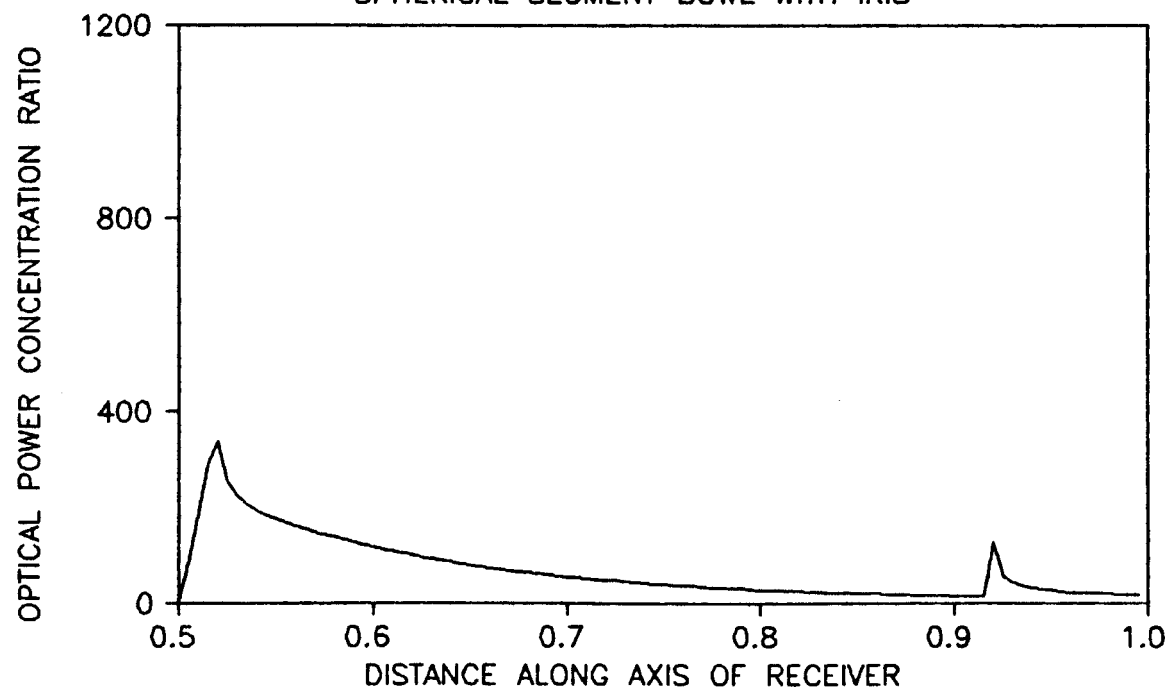
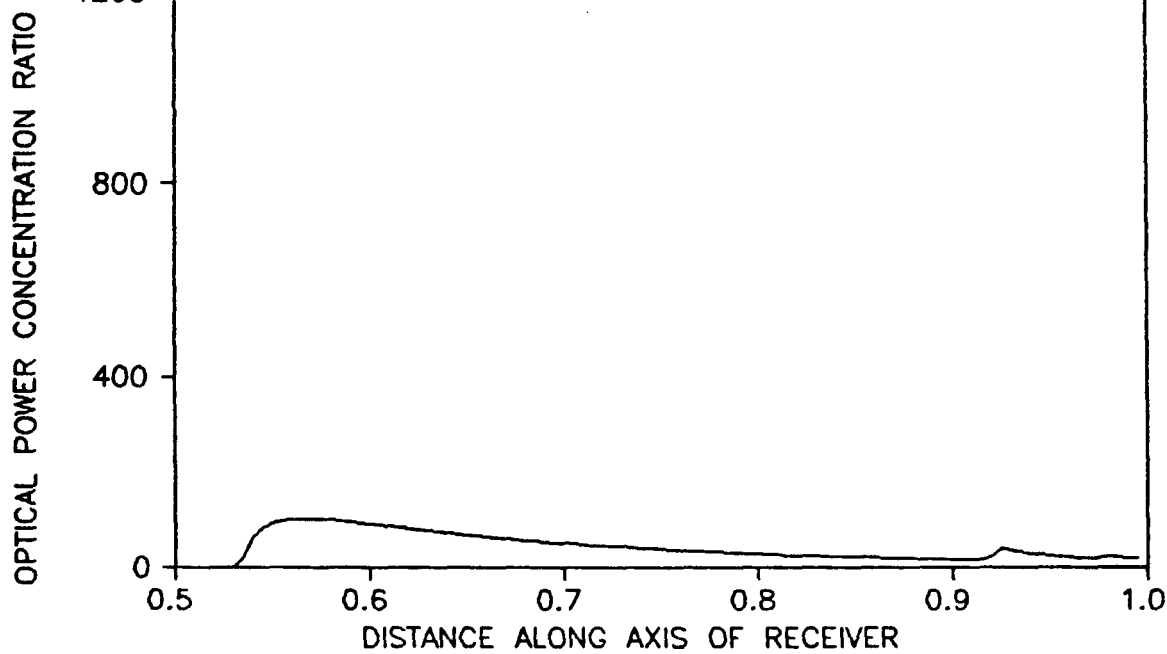


Figure 6.6: Optical Power Concentration for $I = 40^\circ$ and $\theta_R = 30^\circ$, $\theta_I = 45^\circ$, $\phi_0 = 45^\circ$

SPHERICAL SEGMENT BOWL



SPHERICAL SEGMENT BOWL WITH IRIS

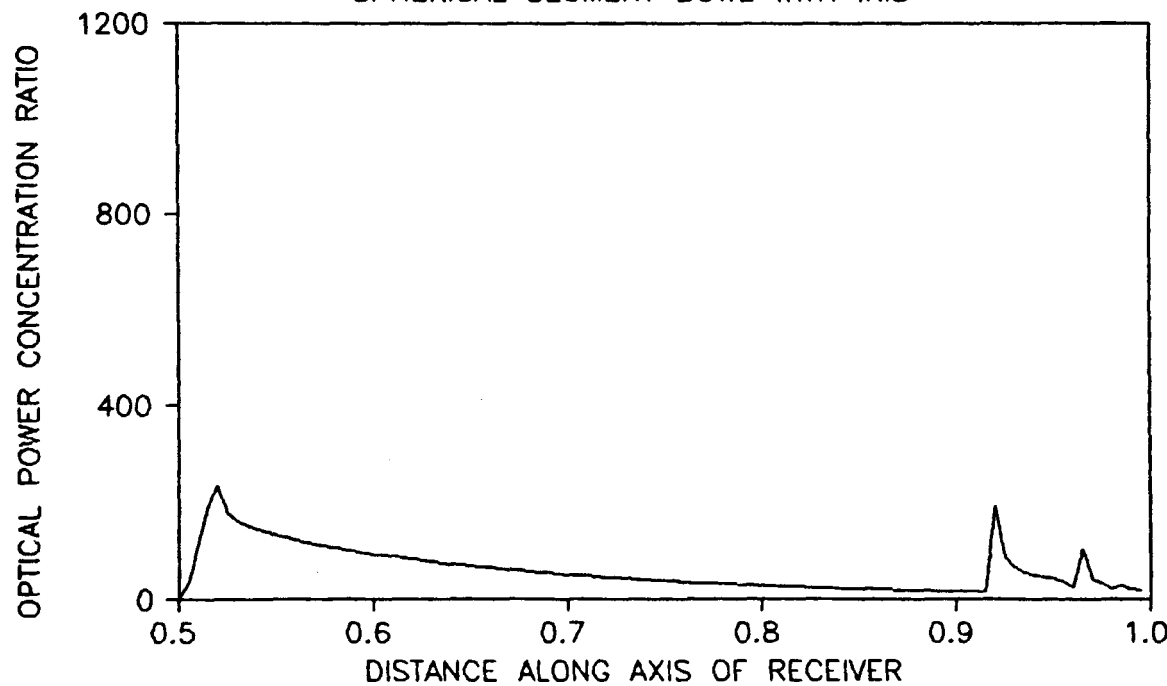


Figure 6.7: Optical Power Concentration for $I = 50^\circ$ and $\theta_R = 30^\circ$, $\theta_I = 45^\circ$, $\phi_0 = 45^\circ$

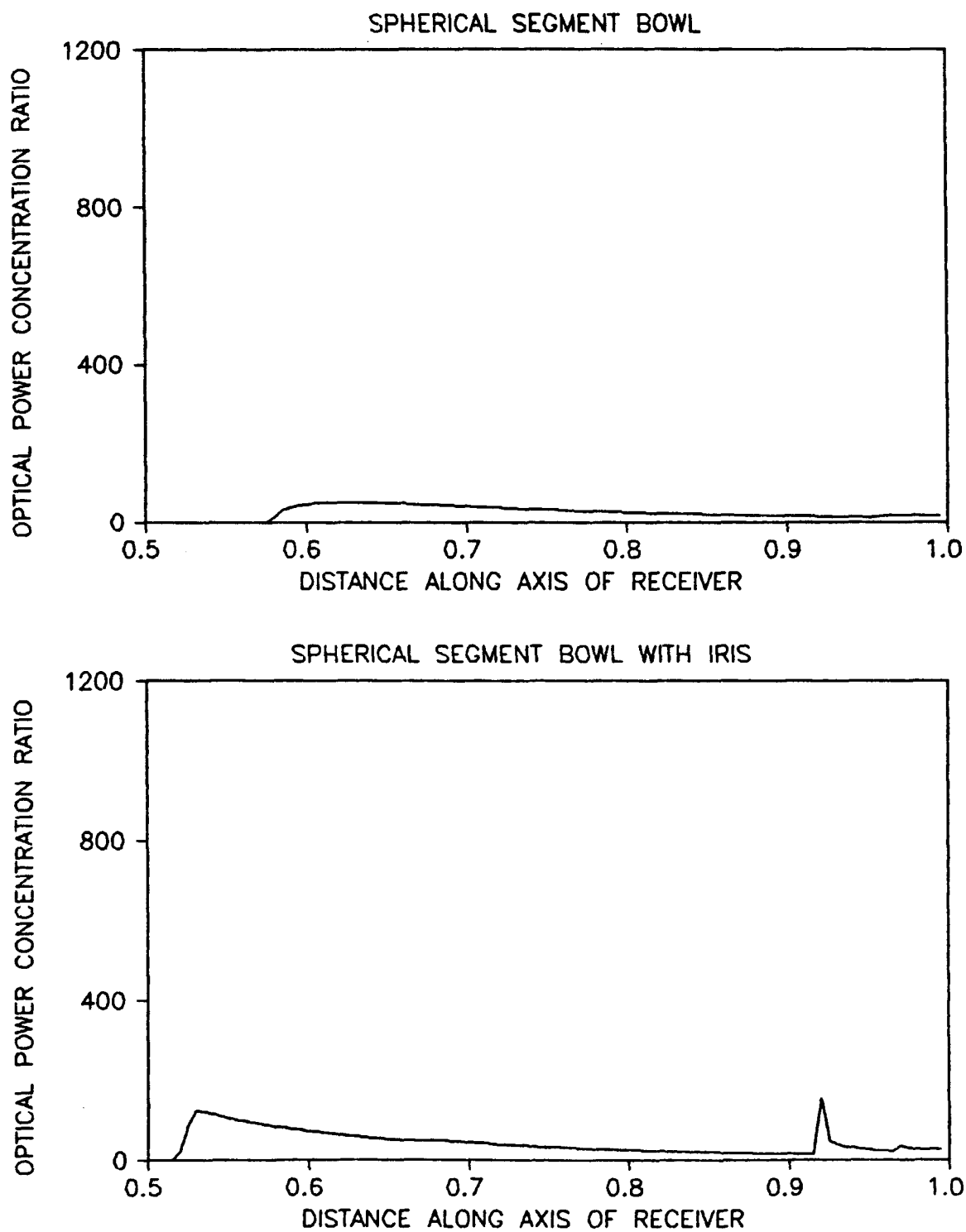
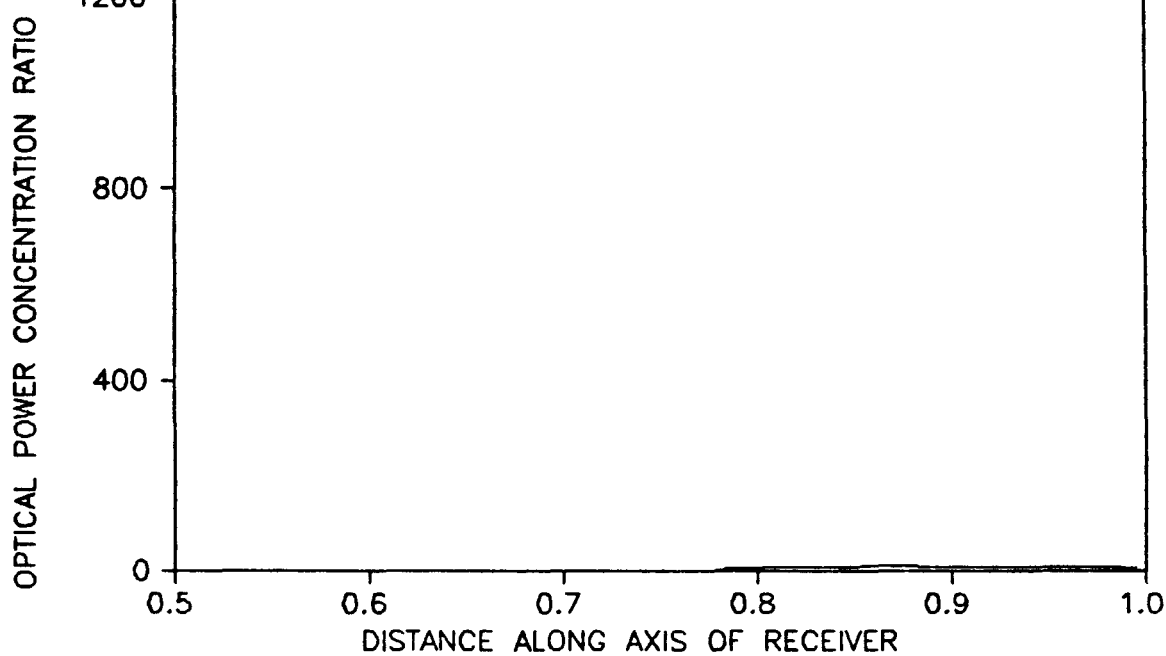


Figure 6.8: Optical Power Concentration for $I = 60^\circ$ and $\theta_R = 30^\circ$, $\theta_I = 45^\circ$, $\phi_0 = 45^\circ$

SPHERICAL SEGMENT BOWL



SPHERICAL SEGMENT BOWL WITH IRIS

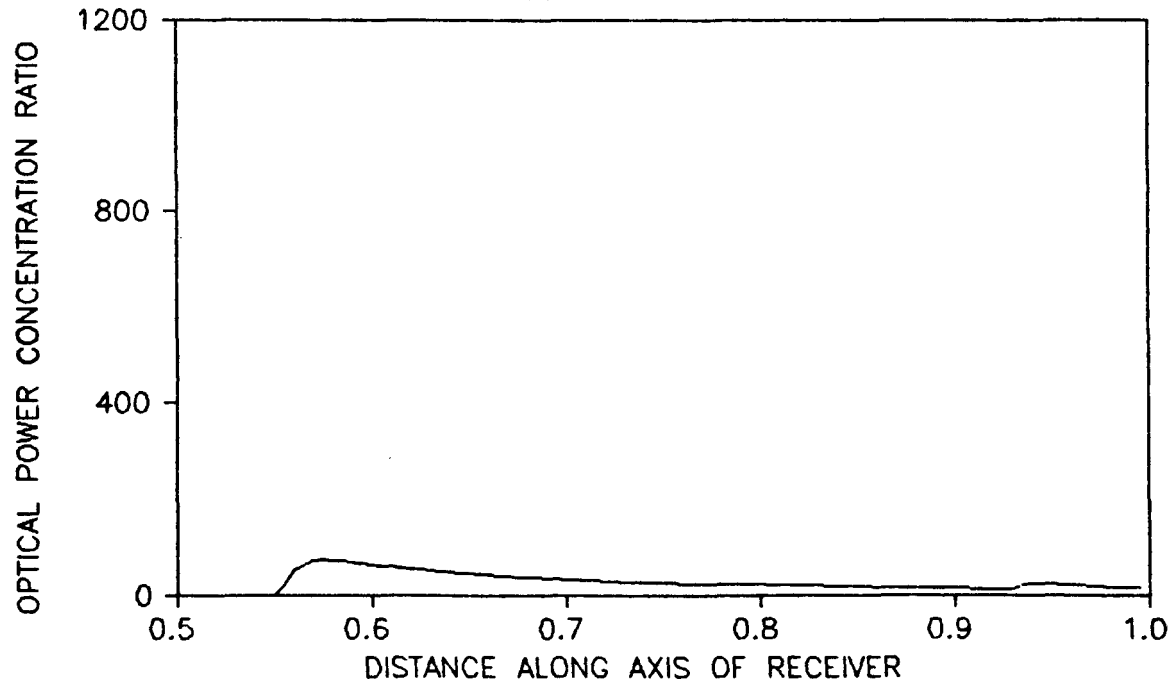


Figure 6.9: Optical Power Concentration for $I = 70^\circ$ and $\theta_R = 30^\circ$, $\theta_I = 45^\circ$, $\phi_0 = 45^\circ$

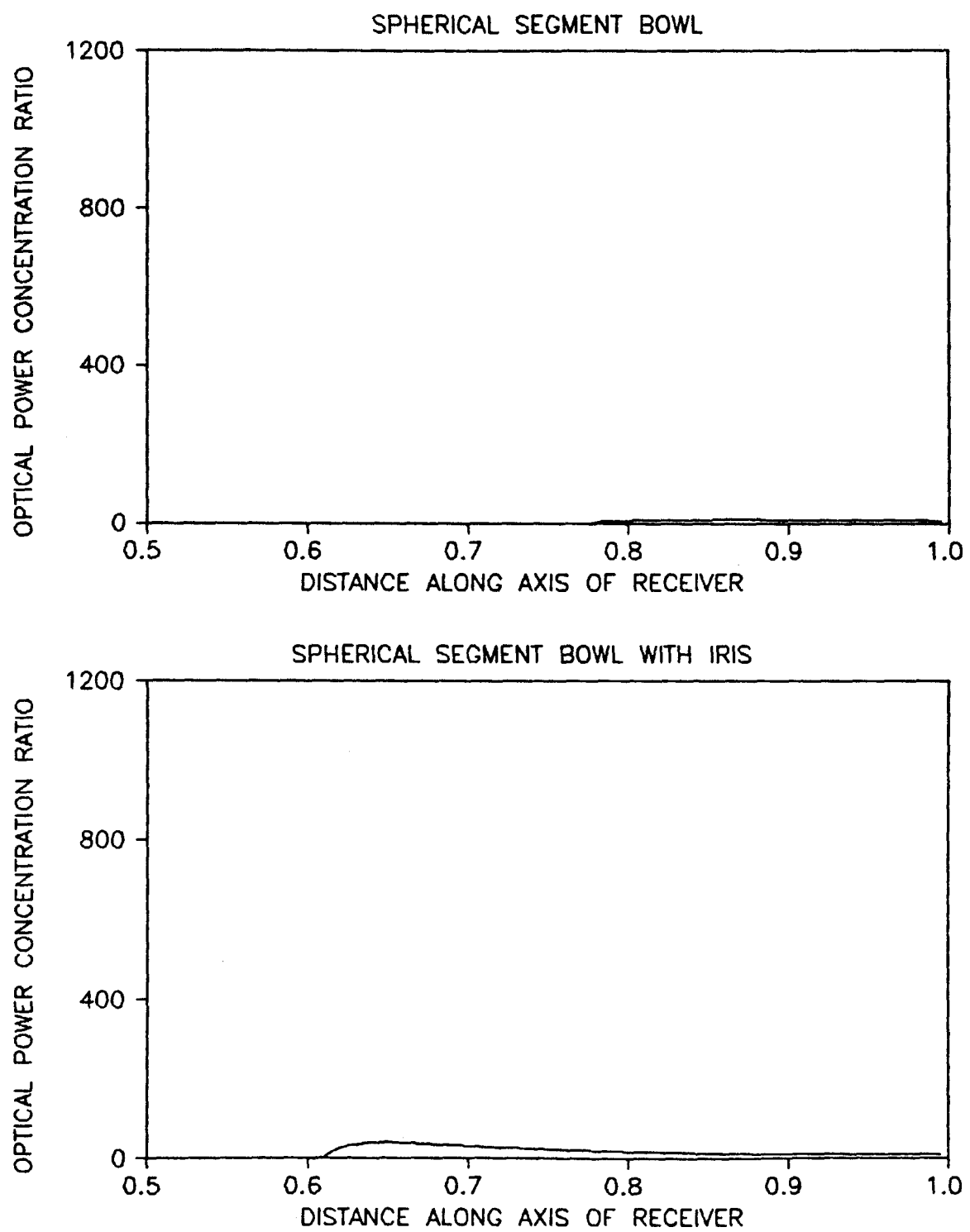


Figure 6.10: Optical Power Concentration for $I = 80^\circ$ and $\theta_R = 30^\circ$, $\theta_I = 45^\circ$, $\phi_0 = 45^\circ$

Bibliography

- [1] Reichert, John D., *A Strategy for Calculations of Optical Concentration Distributions for Fixed Mirror Systems*, Proceedings of the ERDA Solar Workshop on Methods for Optical Analysis for Central Receiver Systems, Houston, Texas, August, 1977, pp. 155-174.
- [2] Reichert, John D., and Brock, Billy C., *Crosbyton Solar Power Project Phase 1 Interim Technical Report*, Texas Tech University, February, 1977, Vol. II, Appendix C, Lubbock, Texas, ERDA Contract No. E(29-2)-3737
- [3] Brock, Billy C., *Optical Analysis of Spherical Segment Solar Collectors*, Texas Tech University, 1977, Lubbock, Texas
- [4] Reichert, John D., Leung, H. and Anderson, Ronald M., *Crosbyton Solar Power Project Phase 1 Interim Technical Report*, Texas Tech University, February, 1978, Vol. V, Appendix C, Lubbock, Texas, US-DOE Contract No. EY-76-C-04-3737
- [5] Leung, H., *Optical Power Concentrations on Aligned and Misaligned Receivers in Solar Power Gridiron Power Systems*, Texas Tech University, Lubbock, Texas, August
- [6] Reichert, John D., Anderson, Ronald M., Ford, Wayne T., White, John T., Brock, Billy C., and Leung, Hipsum, *Analytical Optical Power Concentration Calculations for Reflection from Spherical Mirrors*, Proceedings of the ASME Solar Energy Division Sixth Annual Conference, 1984, pp. 57-63, Las Vegas, Nevada
- [7] Anderson, Ronald M. and Ford, Wayne T., *ROSA: A Computer Model for Optical Power Ratio Calculations*, Technical Information Center,

Office of Scientific and Technical Information, U. S. Department of Energy, July, 1984, Contract Number DOE/AL/21557-T1 (DE85005174)

- [8] Authier, B. and Pouliquen, D., *PERCILES* Proceedings of the ASME Solar Energy Division Fourth Annual Conference, 1982, pp. 150-156, Albuquerque, New Mexico

Appendix A

ROSAIRIS Program Listing

```
C ****
C
C      ROSAIRIS
C      THIS IS A PROGRAM TO CALCULATE THE CONCENTRATION
C      WHEN AN IRIS IS ATTACHED
C
C          WRITTEN BY
C
C          DR. RONALD M. ANDERSON, DEPT. OF MATHEMATICS
C
C          AND
C
C          DR. JOHN D. REICHERT, DEPT. OF ELECTRICAL ENGINEERING
C
C          GRADUATE ASSISTANTS: C. NORWOOD, R. JOHNSTON, C. DAWSON
C
C          TEXAS TECH UNIVERSITY
C          LUBBOCK, TEXAS
C          JULY 24, 1984
C
C          MODIFIED: SEPTEMBER, 1986 BY R. M. ANDERSON
C                      AND M. OBEYESEKERE
C ****
```

```
REAL SUM(100,5),QQ(100),SUMA(100,65,5)
REAL ZSTART(10),ZSTOP(10),PLOTZ(200),PLOTS(200)
COMMON /BLOCKA/ MOMEGA,ISTEPS,OMEGAL(2),OMEGAU(2),XNRML,
*ALPHA,NZ,ZNRML,PSIOS,PSIOC,SIGMAC,
*R31,R32,R33,THTARC,THTAW
COMMON /BLOCKB/ PSIP,PSIPK,PSIM,BETAPK,Q,NBC,
*TNZETA,DRTOP,CSZETA,SNZETA
COMMON /CUT/ THTAR,GAMMAC,ES,A,PHID,GAMMAS,EC,PHIOC,PHIOS
COMMON /GLOBAL/ HALFPI,PI,TWOP,PI,RADIAN
REAL OMEGAL,OMEGAU,XNRML,ZNRML,PSIO,SIGMAC,
*R31,R32,R33,THTARC,THTAW,PSIP,PSIPK,PSIM,BETAPK,Q
COMMON /ENTRY/ R11,R21,R12,R22,R13,R23
COMMON/IRS/HIRIS,TIRIS,S11,S12,S13,S21,S22,S23,S31,S32,S33
INTEGER MOMEGA,ISTEPS,NZ,NBC,KPLOT
INTEGER NZZ(10),ITITLE(6)
REAL A11,A12,A13,A21,A22,A23,A31,A32,A33
REAL BAVG(5),POWER(5),ACONE
```

C

C COORDINATE SYSTEMS USED:

C

C 1. THE S-E-V COORDINATE SYSTEM

C THIS IS THE SOUTH-EAST-VERTICAL COORDINATE SYSTEM
C WHICH IS ALIGNED WITH THE EARTH.

C 2. THE F-G-ES COORDINATE SYSTEM

C THIS COORDINATE SYSTEM IS ALIGNED SO THAT
C THE ES AXIS POINTS TO THE CENTER OF THE SUN.

C 3. THE X-Y-Z COORDINATE SYSTEM

C THIS COORDINATE SYSTEM IS ALIGNED SO THAT
C THE Z AXIS PASSES THROUGH THE CENTER OF
C THE HEMISPHERE AND THE POINT Q ON THE
C RECEIVER AND THE SUN LIES IN THE XZ PLANE.

C 4. THE XR-YR-ZR COORDINATE SYSTEM

C THIS COORDINATE SYSTEM IS ALIGNED SO THAT
C THE ZR AXIS IS THE RECEIVER AXIS OF SYMMETRY.

C 5. THE D-M-A COORDINATE SYSTEM

C THIS COORDINATE SYSTEM IS ALIGNED SO THAT

C THE A AXIS IS THE AXIS OF SYMMETRY OF THE DISH.
C 6. THE DP-MP-AP COORDINATE SYSTEM
C THIS COORDINATE SYSTEM IS OBTAINED BY ROTATING
C THE D-M-A SYSTEM AROUND A-AXIS BY PHIDP, SO THAT
C CENTER OF THE IRIS IS ALIGNED WITH THE DP-AXIS
C
C INPUT VARIABLES
C
C A. ROTATION ANGLE VARIABLES
C PHIRD, PSIRD = THE ROTATION ANGLES, IN DEGREES, BETWEEN THE
C X-Y-Z AND XR-YR-ZR COORDINATE SYSTEMS
C DPSID, DPHID = THE ROTATION ANGLES, IN DEGREES, BETWEEN THE
C F-G-ES AND XR-YR-ZR COORDINATE SYSTEMS
C ED, AD = THE ELEVATION ANGLE AND AZIMUTHAL ANGLE.
C BETWEEN THE S-E-V AND F-G-ES COORDINATE SYSTEMS
C GAMMAD, PHIDD = THE ROTATION ANGLES, IN DEGREES,
C BETWEEN THE S-E-V AND D-M-A
C COORDINATE SYSTEMS
C THTARD = ALTITUDINAL ANGLE, IN DEGREES, BETWEEN
C THE D-M-A AND X-Y-Z COORDINATE SYSTEMS
C
C B. OTHER INPUT VARIABLES
C DPHIRD = THE AMOUNT PHIR IS INCREMENTED IN
C THE PHIR-LOOP (READ IN)
C ISTEPS = THE NUMBER OF INTERVALS USED IN
C THE OMEGA-INTEGRATION
C (USING SIMPSON'S RULE)
C NZZ = NUMBER OF TIMES Z IS INCREMENTED (READ IN)
C REFC = THE REFLECTION COEFFICIENT
C SIGMAD = THE SUN CONE HALF-ANGLE
C SPPHIR = THE FINAL VALUE OF PHIR (READ IN)
C STPHIR = THE STARTING VALUE OF PHIR (READ IN)
C ZSTART = THE INITIAL VALUE OF Z (READ IN)
C ZSTOP = THE FINAL VALUE OF Z (READ IN)
C ZETA=CONE VERTEX HALF-ANGLE
C RTOP=UPPER BOILER RADIUS
C

C TIRIS = CENTRAL ANGE OF THE IRIS
C HIRIS = THE ANGE FROM THE BOTTOM OF THE BOWL TO THE
C TOP OF THE IRIS
C
C
C INTERNAL VARIABLES
C ALPHA = THE ANGLE BETWEEN THE X-AXIS AND THE
C NORMAL TO THE RECEIVER
C COEFF1, COEFF2 = USED TO CALCULATE PHIO
C CONST = A CONSTANT USED IN THE CONCENTRATION FORMULA
C DPSI, DPHI = DPSID, AND DPHID IN RADIANS
C DPSIC, DPHIC = THE COSINES OF DPSI AND DPHI
C DPSIS, DPHIS = THE SINES OF DPSI AND DPHI
C DZ = THE AMOUNT Z IS INCREMENTED EACH TIME THE
C Q-LOOP IS COMPLETED
C DZ DEPENDS ON ZSTART, ZSTOP, AND NZZ
C E, A = ED AND AD IN RADIANS
C EC = THE COSINE OF E
C ES = THE SINE OF E
C GAMMA, PHID = GAMMAD AND PHIDD IN RADIANS
C GAMMAC, PHIDC = THE COSINES OF GAMMA AND PHID
C GAMMAS, PHIDS = THE SINES OF GAMMA AND PHID
C OMEGAL = THE LOWER BOUND ON OMEGA USED IN INTEGRATION
C OMEGAU = THE UPPER BOUND ON OMEGA USED IN INTEGRATION
C PODPC = COS(PHIO-DPHI)
C PODPS = SIN(PHIO-DPHI)
C PSIO, PHIO = THE ROTATION ANGLES BETWEEN THE SUN
C COORDINATE SYSTEM AND THE X-Y-Z COORDINATE SYSTEM
C PSIOC, PHIOC = THE COSINES OF PSIO AND PHIO
C PSIOS, PHIOS = THE SINES OF PSIO AND PHIO
C PSIRD, PHIRD = THE ROTATION ANGLES, IN DEGREES, BETWEEN THE
C XR-YR-ZR AND THE X-Y-Z COORDINATE SYSTEMS
C PSIR, PHIR = PSIRD AND PHIRD IN RADIANS
C PSIRC, PHIRC = THE COSINES OF PSIR AND PHIR
C PSIRS, PHIRS = THE SINES OF PSIR AND PHIR
C Q = THE DISTANCE FROM THE CENTER TO THE POINT
C WHERE THE RAY STRIKES THE RECEIVER

```

C RIMCI (I=1,7) = USED TO COMPUTE THTAZ
C SIGMA = SIGMAD IN RADIANS
C SIGMAC, SIGMAS = THE COSINE AND THE SINE OF SIGMA
C THTAR = THTARD IN RADIANS
C THTARC, THTARS = THE COSINE AND THE SINE OF THTAR
C XNRMAL = THE X-COMPONENT OF THE OUTWARD NORMAL
C           TO THE RECEIVER AT Q
C YNRMAL = THE Y-COMPONENT OF THE OUTWARD NORMAL
C           TO THE RECEIVER AT Q
C XYNRML = PROJECTION OF THE NORMAL TO THE RECEIVER
C           INTO THE XY-PLANE
C XR,YR,ZR = COMPONENTS OF THE NORMAL IN TERMS OF
C           XR-YR-ZR COORDINATE SYSTEM
C Z = THE DISTANCE FROM THE CENTER TO A POINT ON THE
C           CENTRAL AXIS OF THE RECEIVER
C ZNRMAL = THE Z-COMPONENT OF THE OUTWARD NORMAL TO
C           THE RECEIVER AT Q
C
C
C OUTPUT VARIABLES
C LI=NUMBER OF BOUNCES
C QQ = TEMPORARY VARIABLE USED TO PRINT THE VALUE OF Z
C SUM = USED TO COMPUTE THE OMEGA INTEGRAL
C SUMA = USED TO FIND THE TOTAL CONCENTRATION (N=1,5)
C
C
C PROGRAM CONSTANTS
    CALL ERRSET(208,256,-1)
    HALFPI=2.*ATAN(1.)
    PI=2.*HALFPI
    RADIAN=PI/180.
    TWOPI=2.*PI
    MXNP=65
    MXLB=5
C
    DO 14 MM=1,5
    DO 16 NN=1,100

```

```

        SUM(NN,MM)=0.
16      CONTINUE
14      CONTINUE
C
C INPUT VARIABLES
      WRITE(6,208)
208  FORMAT(./././.20X,' INPUT',./.)
      READ(5,197) ITITLE
197  FORMAT(6A4)
      WRITE(6,198) ITITLE
198  FORMAT(11X,6A4./.)
      READ(5,199) DPSID,DPHID
      WRITE(6,202) DPSID,DPHID
      READ(5,299) SIGMAD,ED,AD
      READ(5,299) THTARD,GAMMAD,PHID
      WRITE(6,203) SIGMAD,ED,AD,THTARD,GAMMAD,PHIDD
      WRITE(11,222) ED,AD,GAMMAD
222  FORMAT('ELE =',F10.3,' AZI =',F10.3,' TILT=',F10.3)
199  FORMAT(2F10.5)
299  FORMAT(3F10.5)
202  FORMAT('          BOILER-SUN ALIGNMENT PARAMETERS:./,
*          DELTA PSI (DPSID)      = ',F10.5./,
*          DELTA PHI (DPHID)      = ',F10.5)
203  FORMAT(./,'          SUN PARAMETERS:./,
*          SUN CONE HALF ANGLE (SIGMAD) = ',F10.5./,
*          SUN POSITION:./,
*          ELEVATION (ED)          = ',F10.5./,
*          AZIMUTH (AD)           = ',F10.5./.,
*          DISH PARAMETERS: ./,
*          DISH HALF-ANGLE (THTARD) = ',F10.5./,
*          DISH ALIGNMENT: ./,
*          GAMMAD                  = ',F10.5./,
*          PHID                    = ',F10.5)
      READ(5,399) REFC,ISTEPS
      WRITE(6,204) REFC,ISTEPS
399  FORMAT(F10.5,I5)
204  FORMAT(/.

```

```

*          REFLECTION CONSTANT      = ',F10.5,/
*          ISTEPS                  = ',I5,/
READ(5,1)  STPHIR,SPPHIR,DPHIRD
WRITE(6,205)STPHIR,SPPHIR,DPHIRD
1  FORMAT(3F7.2)
205 FORMAT(
*          START PHIR (STPHIR)      = ',F5.0,/
*          STOP PHIR (SPPHIR)      = ',F5.0,/
1  '        DELTA PHIR (DPHIRD)  = ',F5.2,/
READ(5,2)  NZRR
WRITE(6,206)NZRR
2  FORMAT(I5)
206 FORMAT(
*          NUMBER OF Z-INTERVALS (NZRR) = ',I5)
DO 3 I=1,NZRR
  READ(5,4)  NZZ(I),ZSTART(I),ZSTOP(I)
  WRITE(6,207)I,NZZ(I),ZSTART(I),ZSTOP(I)
4  FORMAT(I5.2F6.3)
207 FORMAT('        FOR I = ',I5,/
*          NUMBER OF Z VALUES    (NZZ)  = ',I5,/
1  '        ZSTART                  =      ',F5.3,/
*          ZSTOP                   =      ',F5.3)
3  CONTINUE
209 FORMAT(
*          ZETAD                  =      ',F5.3,/
*          RTOP                   =      ',F6.4,/)
  ZTOP=ZSTART(1)
  READ(5,11)ZETAD,RTOP
11 FORMAT(2F10.5)
  ZETA=ZETAD*RADIAN
  TNZETA=TAN(ZETA)
  TPSCS=TWOPI/COS(ZETA)
  IF(RTOP.LT.0) RTOP=ZTOP*TNZETA
  WRITE(6,209) ZETAD,RTOP
  DRTOP=RTOP-ZTOP*TNZETA
  CSZETA=COS(ZETA)
  SNZETA=SIN(ZETA)

```

```

      READ(5,499)TIRIS,HIRIS
      WRITE(11,223)THTARD,TIRIS,HIRIS
223  FORMAT('THTAR=',F10.3,' TIRIS=',F10.3,' HIRIS=',F10.3)
499  FORMAT(2F7.2)
      WRITE(6,210)TIRIS,HIRIS
210  FORMAT(/,10X,'IRIS ANGLE(TIRIS)      =',F7.2,/,.
*                  10X,'IRIS HEIGHT ANG(HIRIS)=',F7.2)
C
C CONVERSION FROM DEGREES TO RADIANS
  DPSI=DPSID*RADIAN
  DPHI=DPHID*RADIAN
  PHID=PHIDD*RADIAN
  GAMMA=GAMMAD*RADIAN
  E=ED*RADIAN
  A=AD*RADIAN
  SIGMA=SIGMAD*RADIAN
  THTAR=THTARD*RADIAN
C
C CALCULATION OF TRIG CONSTANTS
  PHIDC=COS(PHID)
  PHIDS=SIN(PHID)
  AMPH=A-PHID
  AMPHC=COS(AMPH)
  AMPHS=SIN(AMPH)
  SIGMAS=SIN(SIGMA)
  SIGMAC=COS(SIGMA)
  EC=COS(E)
  ES=SIN(E)
  GAMMAC=COS(GAMMA)
  GAMMAS=SIN(GAMMA)
  THTARC=COS(THTAR)
  CONST=12.*PI*SIN(.5*SIGMA)**2
  DPSIC=COS(DPSI)
  DPSIS=SIN(DPSI)
  DPHIC=COS(DPHI)
  DPHIS=SIN(DPHI)
C

```

```

C CALCULATION OF ADDITIONAL RIM CONSTANTS FOR ALTERNATE RIM SHAPE
C WHERE A11, A12, . . . , A33 ARE ENTRIES OF THE TRANSITION MATRIX
C ( SEV -> DMA) * (FGES -> SEV)=(F-G-ES)-->(D-M-A)
    A11=GAMMAC*ES*AMPHC + GAMMAS*EC
    A12=-GAMMAC*AMPHS
    A13=GAMMAC*EC*AMPHC - GAMMAS*ES
    A21=ES*AMPHS
    A22=AMPHC
    A23=EC*AMPHS
    A31=ES*GAMMAS*AMPHC-EC*GAMMAC
    A32=-GAMMAS*AMPHS
    A33=EC*GAMMAS*AMPHC+ES*GAMMAC
    D=A13
    XM=A23
    AI=A33
    IF(D**2+XM**2 .EQ. 0.0) THEN
        PHIDP=0.0
    ELSE
        PHIDP=ATAN2(XM,D)
    ENDIF
    PHIDPC=COS(PHIDP)
    PHIDPS=SIN(PHIDP)

C
C FOR MULTIPLE BOUNCES, INITIALIZE ARRAY SUMA
    DO 5009 LBN=1,MXLB
        DO 5019 J1=1,MXNP
            DO 5029 NL=1,100
                SUMA(NL,J1,LBN)=0.
5029    CONTINUE
5019    CONTINUE
5009    CONTINUE
C BEGIN LOOP FOR AZIMUTHAL ANGLE (PHIR)
    PHIRD=STPHIR
C     AREA = 0.0
    JSTOP=1
    IF (DPHIRD .NE. 0.) JSTOP=(SPPHIR-STPHIR)/DPHIRD+1.01
    DO 250 J=1,JSTOP

```

```

PHIR=PHIRD*RADIAN
PHIRC=COS(PHIR)
PHIRS=SIN(PHIR)

C
C BEGINNING OF Z LOOP
DO 600 K=1,NZRR
  Z=ZSTART(K)
  IF(NZZ(K) .LE. 1) GO TO 5000
5001      DZ=(ZSTOP(K)-ZSTART(K))/(NZZ(K)-1)
5000      NZSTOP=NZZ(K)
      DO 3000 NZ=1,NZSTOP
        CALL BOILER(Z,PHIR,PSIR,XR,YR,ZR)
        PSIRC=COS(PSIR)
        PSIRS=SIN(PSIR)

C
C CALCULATION OF PSIO
PSIOC=DPSIC*PSIRC+DPSIS*PSIRS*PHIRC
PSIO=ACOS(PSIOC)
PSIOS=SIN(PSIO)
COEFF1=DPSIC*PSIRS*PHIRC-DPSIS*PSIRC
COEFF2=PSIRS*PHIRS

C
C CALCULATION OF PHI0
IF (ABS(PSIO) .GT. 0.0) GO TO 15
10      PHI0=0.
        GO TO 20
15      PHI0C=DPHIC*COEFF1-DPHIS*COEFF2
        PHI0S=DPHIS*COEFF1+DPHIC*COEFF2
        PHI0=ATAN2(PHI0S,PHI0C)
20      PHI0C=COS(PHI0)
        PHI0S=SIN(PHI0)

C
C CALCULATION OF THE RECEIVER CONSTANTS
PODPC=COS(PHI0-DPHI)
PODPS=SIN(PHI0-DPHI)
ZNRMAL=XR*(PSIOS*DPSIC*PODPC+PSIOC*DPSIS)
*          + YR*PSIOS*PODPS

```

```

1           + ZR*(PSIOS*DPSIS*PODPC-PSIOC*DPSIC)
XNRMAL=XR*(PSIOC*DPSIC*PODPC-PSIOS*DPSIS)
*
1           + YR*PSIOC*PODPS
1           + ZR*(PSIOC*DPSIS*PODPC+PSIOS*DPSIC)
YNRMAL=XR*DPSIC*PODPS - YR*PODPC + ZR*DPSIS*PODPS
XYNRML=SQRT(1.-ZNRMAL**2)
IF (ABS(XYNRML) .LT. .0001 .OR. (ABS(XNRMAL) .LT. .0001
1 .AND. ABS(YNRMAL) .LT. .0001)) GO TO 8526
ALPHA=ATAN2(YNRMAL,XNRMAL)
GO TO 993
8526      ALPHA = 0.0
C
C CALCULATION OF ADDITIONAL RIM CONSTANTS
993      CONTINUE
C CALCULATE THE ENTRIES OF THE TRANSITION MATRIX (X-Y-Z)-->(D-M-A)
C THE 1ST ROW CONTAINS R11,R12,R13, THE 2ND ROW CONTAINS R21,
C R22, R23, AND THE 3RD ROW CONTAINS R31,R32,R33
R11=PSIOC*(PHIOC*A11 + PHI0S*A12) + PSIOS*A13
R12=PHI0S*A11 - PHIOC*A12
R13=PSIOS*(PHIOC*A11 + PHI0S*A12) - PSIOC*A13
R21=PSIOC*(PHIOC*A21 + PHI0S*A22) + PSIOS*A23
R22=PHI0S*A21 - PHIOC*A22
R23=PSIOS*(PHIOC*A21 + PHI0S*A22) - PSIOC*A23
R31=PSIOC*(PHIOC*A31+PHI0S*A32)+PSIOS*A33
R32=PHI0S*A31-PHIOC*A32
R33=PSIOS*(PHIOC*A31+PHI0S*A32)-PSIOC*A33
C
C THE FOLLOWING ARE THE ENTRIES OF THE TRANSITION MATRIX
C FROM (X-Y-Z)-->(DP-MP-AP)
C THESE ARE USED IN THE IRIS ROUTINE
S11=R11*PHIDPC+R21*PHIDPS
S12=R12*PHIDPC+R22*PHIDPS
S13=R13*PHIDPC+R23*PHIDPS
S21=-R11*PHIDPS+R21*PHIDPC
S22=-R12*PHIDPS+R22*PHIDPC
S23=-R13*PHIDPS+R23*PHIDPC
S31=R31

```

```

S32=R32
S33=R33
C
C NOMEGA IS THE NUMBER OF INTERVALS
IF (SIGMA .LT. PSIO) GO TO 40
45      OMEGAL(1)=ALPHA-HALFPI
        OMEGAU(1)=ALPHA+HALFPI
        OMEGAL(2)=ALPHA+HALFPI
        OMEGAU(2)=ALPHA+HALFPI*3.
        NOMEGA=2
        GO TO 90
40      OMEGA1=ACOS(SQRT((SIGMAC**2-PSI0C**2)/PSIOS**2))
        OMEGAU(1)=OMEGA1
        OMEGAL(1)=-OMEGA1
        OMEGAL(2)=PI-OMEGA1
        OMEGAU(2)=PI+OMEGA1
        NOMEGA=2
C
C THE W-INTEGRATION AND THE BETA-INTEGRATION ARE PERFORMED IN
C SUBROUTINE INTGRL. SIMPSON'S RULE IS USED ON THE W-INTEGRATION
90      DO 100 MOMEGA=1,NOMEGA
        CALL INTGRL(SUM)
100     CONTINUE
        QQ(NZ)=Z
3000     Z=Z+DZ
C END OF INTEGRATION-BEGIN PRINT OUT
DO 500 L=1,NZSTOP
C      WRITE(6,501)QQ(L)
      DO 505 LBN=1,MLXB
        SUMA(L,J,LBN)=0.
        SUM(L,LBN)=SUM(L,LBN)/CONST*REFC**LBN
        SUMA(L,J,LBN)=SUMA(L,J,LBN) + SUM(L,LBN)
501      FORMAT('          Z=' ,F8.4)
C      WRITE(6,502)LBN,SUM(L,LBN)
502      FORMAT('          BOUNCE NUMBER='
*           ,I1,'          CONCENTRATION=' ,F14.4)
505      SUM(L,LBN)=0.

```

```

500      CONTINUE
503      FORMAT('
                      TOTAL CONCENTRATION',F14.4,/,/)
                  PHIRD=PHIRD+DPHIRD
250  CONTINUE
      WRITE(6,5280) ITITLE,SIGMAD,ED,AD,
      *                  THTARD,GAMMAD,TIRIS,HIRIS
      WRITE(6,5290)
5280 FORMAT('1',68('='),/,/,/,24X,'SOLAR CONCENTRATION',/,/
      * 5X,6A4.7X,
      * 'SUN HALF-ANGLE =',F7.3,' DEG.',/,5X,
      * 'ELEVATION ANGLE = ',F4.1,' DEG.      AZIMUTH ANGLE = ',
      * F5.1,' DEG.',/,5X,
      * 'DISH HALF-ANGLE = ',F4.1,' DEG.',8X,'TILT ANGLE = ',
      * F4.1,' DEG.',/,8X,
      * 'IRIS OPENING = ',F4.1,' DEG.',7X,'IRIS HEIGHT = ',
      * F4.1,' DEG.',/,/)
5290 FORMAT(1X,68('='),/,8X,'----',16X,'AVERAGE CONCENTRATION',
      *16X,'----',/,3X,'Z',7X,'BOUNCE 1  BOUNCE 2',
      * ' BOUNCE 3  BOUNCE 4  BOUNCE 5  COMBINED',
      * /,1X,68('=')/)
      NLINE=16
      DO 520 LBN=1,MXLB
      POWER(LBN) = 0.
520  CONTINUE
      DO 529 NL=1,NZSTOP
      ACONE=TPSCS*(DRTOP+QQ(NL)*TNZETA)*DZ
      CAVG=0.
      DO 530 LBN=1,MXLB
      AVG=BERGMB(NL,LBN,SUMA)/TWOPI
      BAVG(LBN)=AVG
      CAVG=CAVG+AVG
530  CONTINUE
      NLINE=NLINE+1
      CALL PAGE(NLINE)
      WRITE(6,531) QQ(NL),(BAVG(LBN),LBN=1,MXLB),CAVG
      WRITE(11,5310) QQ(NL),(BAVG(LBN),LBN=1,MXLB),CAVG
531  FORMAT(1X,F6.4,2X,6F10.4)

```

```

5310  FORMAT(F6.4,2X,6F10.4)
      DO 540 LBN=1,MLXB
           POWER(LBN)=POWER(LBN)+BAVG(LBN)*ACONE
540    CONTINUE
529    CONTINUE
      TOTPWR=0.
      DO 543 LBN=1,MLXB
           TOTPWR=TOPWR+POWER(LBN)
543    CONTINUE
      CALL PAGE(NLINE)
      WRITE(6,542)
      WRITE(6,541) (POWER(LBN),LBN=1,MLXB),TOPWR
      WRITE(11,*)'*****'
      WRITE(11,5410) (POWER(LBN),LBN=1,MLXB),TOPWR
541    FORMAT(' TOTAL',/,' POWER ',6F10.4)
5410  FORMAT(8X,6F10.4)
      WRITE(6,542)
542    FORMAT(1X,68('='))
      WRITE(6,8343)
8343  FORMAT('1',/././,'          NORMAL TERMINATION')
      ENDFILE 11
      STOP
      END
C*DECK INTGRL
      SUBROUTINE INTGRL(SUM)
C*** INTGRL PERFORMS THE OMEGA AND BETA INTEGRATIONS
C      AND COMPUTES SUM, WHICH IS RETURNED TO THE
C      MAIN PROGRAM.
C
C***WRITTEN BY:  R.M.ANDERSON, ASSISTED BY CLINT DAWSON
C                  CATHY NORWOOD, AND READ JOHNSTON
C      DATE WRITTEN: 06/01/80
C
C***EXPLANATION OF VARIABLES:
C      BETAL = LOWER LIMIT ON BETA USED IN THE INTEGRATION
C      BETAMI = MINIMUM VALUE OF BETA FOUND WHEN CONSIDERING RIM-CUTOFF
C                  AND SHADOWING EFFECTS

```

```

C  BETAMX = MAXIMUM VALUE OF BETA FOUND WHEN CONSIDERING RIM-CUTOFF
C      AND SHADOWING EFFECTS
C  BETAPK = THE VALUE OF BETA CORRESPONDING TO THE
C      MAXIMUM VALUE OF PSI FOR A GIVEN VALUE OF Q
C  BETASM = BETAL + BETAU
C  BETAT = BETAU - BETAL
C  BETAU = UPPER LIMIT ON BETA USED IN THE INTEGRATION
C  BL = THE LOWER BOUND ON BETA WHEN CONSIDERING THE RELATIONSHIP
C      BETWEEN BETA, PSIP, AND PSIM
C  BU = THE UPPER BOUND ON BETA WHEN CONSIDERING THE RELATIONSHIP
C      BETWEEN BETA, PSIP, AND PSIM
C  CONSTW = A CONSTANT USED IN THE OMEGA INTEGRATION
C  DOMEGA = (OMEGAU - OMEGAL)/ISTEPS
C  ETA, BETA = USED TO COMPUTE PSIP AND PSIM
C  NBC, XN = THE NUMBER OF BOUNCES
C  OMEGA = THE AZIMUTHAL ANGLE MEASURED CLOCKWISE FROM THE X-AXIS
C  PSIM = ANGLE BETWEEN THE RECEIVER AND THE
C      LEFT EDGE OF THE SUN CONE IN THE
C      PLANE OMEGA=CONSTANT
C  PSIP = ANGLE BETWEEN THE RECEIVER AND THE
C      RIGHT EDGE OF THE SUN CONE IN THE
C      PLANE OMEGA=CONSTANT
C  PSIPK = MAXIMUM VALUE OF PSI FOR A GIVEN N AND Q
C  QSBETA = Q TIMES THE SINE OF BETAPK
C  RHO = USED TO FIND BETAMX TO ASSURE THAT THE DOT PRODUCT IS
>= 0
C  SB = USED TO COMPUTE THE BETA-INTEGRAL
C  SUM1 = USED TO COMPUTE THE BETA INTEGRAL
C  THTAW = USED TO COMPUTE THTAZP
C  THTAZ = USED TO FIND THTAZP AND THTAZM
C  THTAZE = THETA-EFFECTIVE, USED TO COMPUTE BETAMX
C  THTAZM = THE ANGLE BETWEEN THE RECEIVER AND THE LEFT RIM
C  THTAZP = THE ANGLE BETWEEN THE RECEIVER AND THE RIGHT RIM
C
C*****
REAL SUM(100,5)
REAL BL(2),BU(2)

```

```

INTEGER NBETA
COMMON /BLOCKA/ MOMEGA,ISTEPS,OMEGAL(2),OMEGAU(2),XYNRML,
* ALPHA,NZ,ZNRMAL,PSIOS,PSIOC,SIGMAC,
* R31,R32,R33,THTARC,THTAW,TIRIS,HIRIS
COMMON /BLOCKB/ PSIP,PSIPK,PSIM,BETAPK,Q,NBC,
* TNZETA,DRTOP,CSZETA,SNZETA
COMMON /CUT/ THTAR,GAMMAC,ES,A,PHID,GAMMAS,EC,PHIOC,PHIOS
COMMON /GLOBAL/ HALFPI,PI,TWOP,PI,RADIAN
C THE W-INTEGRATION--ISTEPS IS THE NUMBER OF
C INTEGRATION STEPS/INTERVAL
C SIMPSON'S RULE IS USED
UNIT=-1.
DOMEWA=(OMEGAU(MOMEGA)-OMEGAL(MOMEGA))/ISTEPS
DO 101 I=2,ISTEPS
OMEGA=OMEGAL(MOMEGA)+(I-1)*DOMEWA
OMEGAC=COS(OMEGA)
CONSTW=(3.-UNIT)*DOMEWA
OMEGAS=SIN(OMEGA)
RHO=ATAN2(XYNRML*COS(OMEGA-ALPHA),ZNRMAL)
C
C CALCULATION OF PSIM,PSIP
ETA=ATAN2(PSIOS*OMEGAC,PSIOC)
BETA=ACOS(SIGMAC/SQRT(PSIOC**2+(PSIOS*OMEGAC)**2))
PSIP=ETA+BETA
PSIM=ETA-BETA
C
C CALCULATION OF EFFECTIVE RIM ANGLE PARAMETERS
C**** THIS IS TO FIND THETAZ-PLUS AND THETAZ-MINUS
C WHEN AN IRIS IS ATTACHED TO THE USUAL DISH
CALL IRIS(OMEGA,THTAZP,THTAZM,IFLAG)
IF (IFLAG .EQ. 1) GO TO 101
IF (THTAZP .LE. 0.0) GO TO 101
THTAZM=AMAX1(0.,THTAZM)
THTAZP=AMIN1(THTAZP,PI-THTAZP-PSIP-PSIM)
IF (THTAZP .LE. THTAZM) GO TO 101
C
C CALCULATION OF MINIMUM AND MAXIMUM BETA AND EFFECTIVE RIM ANGLE

```

```

C BETAMI,BETAMX AND THTAZE,RESPECTIVELY
      BETAMI=0.
      IF (THTAZM .LE. 0.0) GO TO 302
      BETAMI=ATAN2(SIN(THTAZM),(COS(THTAZM)-Q))
302      BETAMI = AMAX1(BETAMI,-HALFPI+RHO)
      DO 370 NBC=1,5
      XN=NBC
      THTAZE=(2.*XN-1.)*THTAZP+(XN-1.)*(PSIP+PSIM-PI)
      IF ((THTAZE-THTAZM) .LE. 0.0) GO TO 300
      BETAMX=ATAN2(SIN(THTAZE),(COS(THTAZE)-Q))
      BETAMX=AMIN1(BETAMX,PI,HALFPI+RHO)

C
C CALCULATION OF BETA-PEAK AND PSI-PEAK
      IF (Q .GT. .5) GO TO 305
      IF(NBC .GT. 1) GO TO 305
      BETAPK=0.0
      PSIPK=0.0
      GO TO 306
305      QSBETA=SQRT(((2.*XN*Q)**2-1.)/((2.*XN)**2-1.))
      BETAPK=ASIN(QSBETA/Q)
      PSIPK = 2.*XN*ASIN(QSBETA)-BETAPK-(XN-1.)*PI

C
C CONSIDERATION OF THE RELATIONSHIP BETWEEN PSIM,PSIP,PSIPK
306      IF (PSIM .GE. PSIPK) GO TO 300
      CALL BLIMIT(BL,BU,NBETA)

C
C TEST INTERVALS OF INTEGRATION FOR RIM EFFECTS
      SUM1=0.
      DO 360 MBETA=1,NBETA
      BETAL=AMAX1(BL(MBETA),BETAMI)
      BETAU=AMIN1(BU(MBETA),BETAMX)
      BETAT=BETAU-BETAL
      BETASM=BETAU+BETAL
      IF (BETAT .LE. 0.0) GO TO 360
      SB=.5*(BETAT-SIN(BETAT)*
      COS(BETASM))*COS(OMEGA-ALPHA)
      SUM1=SUM1+.5*ZNRMAL*SIN(BETAT)

```

```

* *SIN(BETASM)+SB*XYNRML
360      CONTINUE
370      SUM(NZ,NBC)=SUM(NZ,NBC)+SUM1*CONSTW
300      CONTINUE
101      UNIT=-UNIT
      RETURN
      END
C*DECK SOLN
      FUNCTION SOLN(BETA,PSI)
C*** FUNCTION SOLN COMPUTES BL AND BU USING NEWTON'S METHOD
C
C***WRITTEN BY:  R.M.ANDERSON
C***DATE WRITTEN: 06/01/80
C
C***EXPLANATION OF VARIABLES
C  BETA = FIRST GUESS FOR SOLN
C  PSI = BETA - (2*NBC*SIN(Q*SIN(BETA)) + (NBC-1)*PI
C  Q = VECTOR FROM CENTER OF DISH TO POINT ON THE RECEIVER
C  NBC = BOUNCE NUMBER
C
      COMMON /BLOCKB/ PSIP,PSIPK,PSIM,BETAPK,Q,NBC,
      *           TNZETA,DRTOP,CSZETA,SNZETA
      COMMON /GLOBAL/ HALFPI,PI,TWOPI,RADIAN
      A=BETA
      B=PSI
      XN=NBC
      B=B+(XN-1.)*PI
      DO 10 I=1,30
      QAS=Q*SIN(A)
      DELA=(B-2.*XN*ASIN(QAS)+A)/(1.-2.*Q*XN*COS(A)/
      * SQRT(1.-QAS**2))
      A=A-DELA
      IF (ABS(DELA) .LE. .0001) GO TO 300
11      IF (A .LT. 0.0) GO TO 200
12      IF (A .GT. PI) GO TO 200
10      CONTINUE
      WRITE(6,100)

```

```

100  FORMAT(' ITERATION DID NOT CONVERGE')
    GO TO 300
200  WRITE(6,201)
201  FORMAT(' ITERATION DIVERGED')
    A=0.
300  SOLN=A
    RETURN
    END
C*DECK BLIMIT
    SUBROUTINE BLIMIT(BL,BU,NBETA)
C
    REAL BL(2),BU(2)
    INTEGER NBETA
    COMMON /BLOCKB/ PSIP,PSIPK,PSIM,BETAPK,Q,NBC,
    *                  TNZETA,DRTOP,CSZETA,SNZETA
    COMMON /GLOBAL/ HALFPI,PI,TWOPi,RADIAN
C**** CONSIDERATION OF THE RELATIONSHIP BETWEEN PSIM,PSIP,PSIPK
C      IN ORDER TO DETERMINE THE BETA-LIMITS OF INTEGRATION
C
C***WRITTEN BY: R.M. ANDERSON, ASSISTED BY CLINT DAWSON,
C                  CATHY NORWOOD, AND READ JOHNSTON
C***DATE WRITTEN: 06/01/83
C
C***EXPLANATION OF VARIABLES:
C  BL(2) = ARRAY CONTAINING LOWER BETA-LIMITS
C  BU(2) = ARRAY CONTAINING UPPER BETA-LIMITS
C  NBETA = NUMBER OF BETA-REGIONS OVER WHICH TO INTEGRATE
C          NBETA=1 OR 2
C  BETA = THE FIRST GUESS FOR BL(I) OR BU(I) TO BE
C          USED IN SUBROUTINE SOLN
C
    IF (PSIM .LT. 0.0) GO TO 320
C
C  PSIM >=0
    IF (PSIP .LT. PSIPK) GO TO 315
C
C  PSIM >=0 AND PSIP>=PSIPK

```

```

G1=SQRT((PSIPK-PSIM)/(PSIPK+(NBC-1)*PI))
BETA=BETAPK*(1.-G1)
BL(1)=SOLN(BETA,PSIM)
BETA=BETAPK*(1.+G1)
BU(1)=SOLN(BETA,PSIM)
NBETA=1
GO TO 350
C
C PSIM>=0 AND PSIP<PSIPK
315   G1=SQRT((PSIPK-PSIM)/(PSIPK+(NBC-1)*PI))
      G2=SQRT((PSIPK-PSIP)/(PSIPK+(NBC-1)*PI))
      BETA=BETAPK*(1.-G1)
      BL(1)=SOLN(BETA,PSIM)
      BETA= BETAPK*(1.-G2)
      BU(1)=SOLN(BETA,PSIP)
      BETA=BETAPK*(1.+G2)
      BL(2)=SOLN(BETA,PSIP)
      BETA=BETAPK*(1.+G1)
      BU(2)=SOLN(BETA,PSIM)
      NBETA=2
      GO TO 350
C
C PSIM<0
320 IF (PSIP .GT. PSIPK) GO TO 325
      IF (PSIP .GT. 0.0) GO TO 323
C
C PSIM<0 AND PSIP<=0 AND SINGLE BOUNCE
322   IF (NBC .GT. 1) GO TO 391
390   G1=SQRT((PSIP-PSIPK)/(-(NBC*PI+PSIPK)))
      G2=SQRT((PSIM-PSIPK)/(-(NBC*PI+PSIPK)))
      BETA=BETAPK+(PI-BETAPK)*G1
      BL(1)=SOLN(BETA,PSIP)
      BETA=BETAPK+(PI-BETAPK)*G2
      BU(1)=SOLN(BETA,PSIM)
      NBETA=1
      GO TO 350
C

```

```

C PSIM<0 AND PSIP<=0 AND MULTIPLE BOUNCE
391      BL(1)=SOLN(0.,PSIM)
          BU(1)=SOLN(BL(1),PSIP)
          G1=SQRT((PSIP-PSIPK)/(-(NBC*PI+PSIPK)))
          BETA=BETAPK+(PI-BETAPK)*G1
          BL(2)=SOLN(BETA,PSIP)
          BU(2)=SOLN(BL(2),PSIM)
          NBETA=2
          GO TO 350

C
C PSIM<0 AND 0<=PSIP<=PSIPK
323      BL(1)=0.
          IF (NBC .LE. 1) GO TO 374
          BL(1)=SOLN(0.,PSIM)
374      G1=SQRT((PSIPK-PSIP)/(PSIPK+(NBC-1)*PI))
          BETA=BETAPK*(1.-G1)
          BU(1)=SOLN(BETA,PSIP)
          BETA=BETAPK*(1.+G1)
          BL(2)=SOLN(BETA,PSIP)
          G2=SQRT((PSIM-PSIPK)/(-(NBC*PI+PSIPK)))
          BETA=BETAPK+(PI-BETAPK)*G2
          BU(2)=SOLN(BETA,PSIM)
          NBETA=2
          GO TO 350

C
C PSIM<0 AND PSIP>PSIPK
325      BL(1)=0.
          IF (NBC .LE. 1) GO TO 376
          BL(1)=SOLN(0.,PSIM)
376      G1=SQRT((PSIM-PSIPK)/(-(NBC*PI+PSIPK)))
          BETA=BETAPK+(PI-BETAPK)*G1
          BU(1)=SOLN(BETA,PSIM)
          NBETA=1
350      RETURN
          END
C*DECK BOILER
          SUBROUTINE BOILER(Z,PHIR,PSIR,XR,YR,ZR)

```

```

C
C*** GENERAL BOILER SUBROUTINE.
C
COMMON /BLOCKB/ PSIP,PSIPK,PSIM,BETAPK,Q,NBC,
*                  TNZETA,DRTOP,CSZETA,SNZETA
COMMON /GLOBAL/ HALFPI,PI,TWOPI,RADIAN
C
RADIUS=DRTOP+Z*TNZETA
Q=SQRT(RADIUS**2+Z**2)
PSIR=ATAN2(RADIUS,Z)
XR=COS(PHIR)*CSZETA
YR=SIN(PHIR)*CSZETA
ZR=SNZETA
RETURN
END
C*DECK IRIS
SUBROUTINE IRIS(OMEGA,THTAZP,THTAZM,IFLAG)
C THIS ROUTINE WILL COMPUTE THTAZP AND THETAZM FOR A GIVEN
C OMEGA ANGLE. THE RIM ANGLE OF THE DISH IS THTAS(1)
C AND THE RIM ANGLE OF THE IRIS IS THTAS(2)
C
C WRITTEN BY
C     DR. R. M. ANDERSON
C AND
C     M. N. OBEYESEKERE
C WRITTEN ON: 5/18/86
C
C
REAL THTAS(2),FIRPLS,FIRMNS,ARG
COMMON /ENTRY/ R11,R21,R12,R22,R13,R23
COMMON /CUT/ THTAR,GAMMAC,ES,A,PHID,GAMMAS,EC,PHIOC,PHIOS
COMMON /BLOCKA/ MOMEGA,ISTEPS,OMEGAL(2),OMEGAU(2),XYNRML,
*ALPHA,NZ,ZNRMAL,PSIOS,PSIOC,SIGMAC,
*R31,R32,R33,THTARC,THTAW
COMMON /GLOBAL/ HALFPI,PI,TWOPI,RADIAN
COMMON/IRS/HIRIS,TIRIS,S11,S12,S13,S21,S22,S23,S31,S32,S33
IFLAG=0

```

```

TEST=0.0
OMEGAC=COS(OMEGA)
OMEGAS=SIN(OMEGA)
THTARC=COS(THTAR)
THTARS=SIN(THTAR)
PHIZRO=TIRIS*RADIAN*0.5
THTAS(1)=THTAR
THTAS(2)=HIRIS*RADIAN
DEN=SQRT((S31*OMEGAC+S32*OMEGAS)**2+S33**2)
IF(DEN.EQ.0.0)THEN
  IFLAG=1
  RETURN
END IF
ARG=COS(THTAS(2))/DEN
IF(ABS(ARG).GT.1.0)THEN
  IFLAG=1
  RETURN
END IF
THTABI=ACOS(ARG)
THTAA=ATAN2(-(S31*OMEGAC+S32*OMEGAS),-S33)
THTAZM=AMAX1(0.0,(THTAA-THTABI))
THTAZ =THTAA+THTABI
UP=(S21*OMEGAC+S22*OMEGAS)*SIN(THTAZ)+S23*COS(THTAZ)
DWN=(S11*OMEGAC+S12*OMEGAS)*SIN(THTAZ)+S13*COS(THTAZ)
PHII=ATAN2(UP,DWN)
IF(ABS(PHII).GT.(PI-PHIZRO))THEN
  THTAZP=THTAZ
  RETURN
END IF
ARG=COS(THTAS(1))/DEN
IF(ARG.GT.1.0)THEN
  IF(PHII.LE.0.0)THEN
    PHIR=PI+PHIZRO
  ELSE
    PHIR=PI-PHIZRO
  END IF
  PHIRS=SIN(PHIR)

```

```

PHIRC=COS(PHIR)
A2=S21*OMEGAC+S22*OMEGAS
A1=S11*OMEGAC+S12*OMEGAS
THTAZ=ATAN((S23*PHIRC-S13*PHIRS)/(A1*PHIRS-A2*PHIRC))
THTAZP=THTAZ
ELSE
    THTAZP=THTAA+ACOS(ARG)
END IF
90  RETURN
END

C
C
C* DECK TRAP
C(THIS IS USED ONLY IF AREA NEEDS TO BE COMPUTED)
    REAL FUNCTION TRAP(N,DX,F)
C
C PURPOSE: THIS ROUTINE COMPUTES THE TOTAL CONCENTRATION OF SINGLE
C           BOUNCE BY USING TRAPEZOID RULE
C DATE WRITTEN: 31/03/86
C AUTHOR: KIM HSU
C
    REAL F(N)
C
        S = 0.0
        M = N-1
        DO 10 I = 2,M
            S = S + F(I)*2.0
10    CONTINUE
        S = S + F(1) + F(N)
        TRAP = DX*S/2.0
        RETURN
        END

C*DECK BERGMB
C
    REAL FUNCTION BERGMB(NL,LB,SUMA)
C
C VARIABLES:

```

```

C      LB      THE NUMBER OF BOUNCE
C      NL      THE SUBSCRIPT OF Z
C
COMMON /GLOBAL/ HALFPI,PI,TWOPI,RADIAN
REAL SUMA(100,65,5)
INTEGER NL
REAL RMBS(5)
DO 10 K=1,5
  LJ=1
  RMBS(K)=0
  ISTOP=2**K
  H=TWOPI/FLOAT(ISTOP)
  DO 20 I=1,ISTOP
    RMBS(K)=H*SUMA(NL,LJ,LB) + RMBS(K)
    LJ=LJ + 32/ISTOP
20  CONTINUE
10  CONTINUE
  KOUNT=0
  DO 30 J=1,4
    KOUNT=KOUNT+1
    CALL ACCEL(KOUNT,J,RMBS)
30  CONTINUE
  BERGMB=RMBS(1)
  RETURN
  END
C*DECK ACCEL
  SUBROUTINE ACCEL(KOUNT,J,RSUM)
  REAL RSUM(5)
  INTEGER KOUNT,J
  JSTOP=5-J
  DO 10 J1=1,JSTOP
    RSUM(J1)=(4**KOUNT*RSUM(J1+1) - RSUM(J1))/(4**KOUNT-1)
10  CONTINUE
  RETURN
  END
C*DECK PAGE
C

```

```
SUBROUTINE PAGE(LINE)
C
C PURPOSE: CONTROL PAGE LENGTH OF THE OUTPUT PAGE
C DATE WRITTEN: 06/01/86
C AUTHOR: KIM T. HSU
C VARIABLES:
C           LINE   INPUT IS THE CURRENT NUMBER OF LINES. IF LINE
C           IS GREATER THAN 51 THEN IN RETURN LINE IS
C           EQUAL TO 6
C
IF(LINE.LE.51) GOTO 10
      WRITE(6,1000)
      WRITE(6,2000)
      LINE= 6
1000  FORMAT(1X,68('='),/, '1', 'CONTINUE... ')
2000  FORMAT(1X,68('='),/,8X,'----',16X,'AVERAGE CONCENTRATION',
           *16X,'----',/,.3X,'Z',7X,'BOUNCE 1  BOUNCE 2',
           * ' BOUNCE 3  BOUNCE 4  BOUNCE 5  COMBINED',
           * /,1X,68('=')/)
10  RETURN
      END
```

BOILER SHAPE: CONE

0.	0.	
0.267	60.	30.0
30.	15.	00.0
1.00		50
0.0	360.00	11.25
	1	
100	.5	.995
0.267		-1.0
90.0		45.0